약학박사학위논문

GATA-2 의존적인 c-Kit^{+}CD24^{+} 자연 살해 세포의 골수성 세포로의 전환에 대한 연구

Studies on GATA-2-dependent lineage reprogramming of c-Kit^{+}CD24^{+} natural killer cells into myeloid cells

2019 년 10 월

서울대학교 대학원

분자의학 및 바이오 제약학과 면역학 전공

송 보 영

Abstract

Studies on GATA-2-dependent lineage reprogramming of c-Kit^{+}CD24^{+} natural killer cells into myeloid cells

Boyeong Song

Laboratory of Immunology

Department of Molecular Medicine and Biopharmaceutical Sciences

The Graduate School

Seoul National University

Although previous studies showed that manipulating lineage determinants causes *in vitro* lineage reprogramming in immune cells, naturally occurring lineage conversion is still poorly understood in both homeostasis and diseases. Myeloid progenitor cells have generally been considered the exclusive source of myeloid cells under steady-state conditions.

Here I show that NK cells contributed to a myeloid cell lineage pool in naïve and tumor-bearing mice. By using fate tracing of NKp46^{+} cells, I found that myeloid cell populations could be derived from NK-committed NKp46^{+} cells. Notably, among mature CD11b^{+}CD27^{+} NK cells, c-Kit^{+}CD24^{+} NK cells were capable of differentiating into a range of myeloid lineages *in vitro* and reprogrammed into neutrophils and monocytes *in vivo*. The differentiation was completely inhibited by NK-stimulating cytokines. In addition to the potential for lineage conversion, c-Kit^{+}CD24^{+} NK cells retained NK cell phenotypes and effector functions. Mechanistically, GATA-2 was necessary for the differentiation of the c-Kit^{+}CD24^{+} NK cells into myeloid cells. Therefore, I discovered that GATA-2-dependent conversion of c-Kit^{+}CD24^{+} NK cells contributes to myeloid cell development and identified a novel pathway for myeloid lineage commitment in physiological conditions. My findings provide deep and novel insight for understanding the myeloid cell development.

Keywords: Lineage Reprogramming, Myeloid Cell Development, Natural Killer Cell, c-Kit, CD24, GATA-2

Student number: 2011-24245

Table of Contents

List of Figures and Tables

Abbreviations

ALL	Acute lymphoblastic leukemia
AML	Acute myeloid leukemia
BFU-E	Burst forming unit-erythroid
BM	Bone marrow
CD	Cluster of differentiation
cDC	Conventional dendritic cell
CFU-GEMM	Colony-forming unit-granulocyte, erythrocyte, macrophage, megakaryocyte
CFU-GM	Colony-forming unit-granulocyte, macrophage
CFU-G	Colony-forming unit-granulocyte
CFU-M	Colony-forming unit-macrophage
CLP	Common lymphoid progenitor
CMP	Common myeloid progenitor
DC	Dendritic cell
DEG	Differentially expressed gene
EYFP	Enhanced yellow fluorescent protein
FACS	Fluorescence-activated cell sorting
GFP	Green fluorescent protein

GMP	Granulocyte-macrophage progenitor
HSPC	Hematopoietic stem and progenitor cell
IFN-γ	Interferon-gamma
IL	Interleukin
iNKT	Invariant natural killer T cell
MDSC	Myeloid-derived suppressor cell
mo-DC	Monocyte-derived dendritic cell
NK cell	Natural killer cell
pDC	Plasmacytoid dendritic cell
PI	Propidium iodide
TBM	Tumor-bearing mice

Introduction

I. Hematopoiesis

Hematopoiesis is a process by which blood cellular components were produced. In the classical hematopoietic pathway [1-3], hematopoietic stem cells diverge into common lymphoid progenitors (CLPs) and common myeloid progenitors (CMPs). CLPs give rise to lymphocytes, including natural killer cells (NK cells), and CMPs further develop into two restricted progenitor lines: those for granulocytes and monocyte/macrophages and those for erythrocytes and megakaryocytes (**Figure 1**).

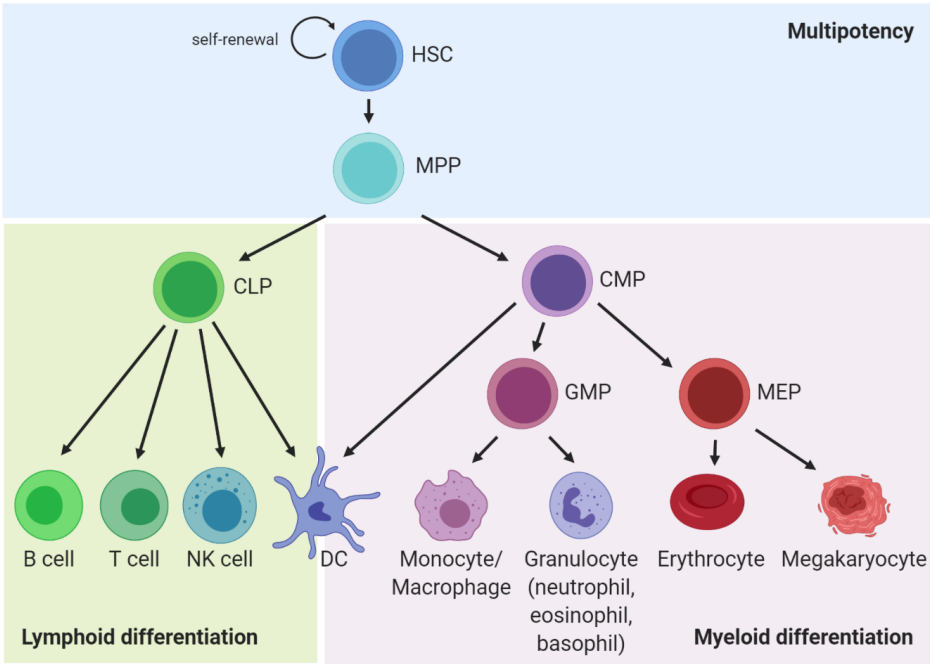

Figure 1. The classical model of hematopoiesis

Hematopoietic stem cells reside at the top of hematopoietic hierarchy and produce terminally differentiated blood cells through sequential differentiation along multipotent and oligopotent progenitors. According to the classical concept of hematopoiesis, common lymphoid progenitors (CLPs) and common myeloid progenitors (CMPs) represented the first lineage bifurcation in the lineage tree. CLPs differentiate into T, B, and natural killer (NK), and innate lymphoid cells, whereas CMPs generate myeloid lineage cells. HSC, hematopoietic stem cell; MPP, multipotent progenitor; CMP, common myeloid progenitor; CLP, common lymphoid progenitor; MEP, megakaryocyte erythroid progenitor; GMP, granulocyte macrophage progenitor. (Modified from Avgustinova & Benita, Nature Reviews Molecular Cell Biology 17, 643-658 (2016) [4] & Ackermann et al., *EMBO Molecular Medicine* 7, 1388-1402 (2015) [5])

II. Lineage Reprogramming of immune cells

The lineage commitment was first thought to be a stepwise and irreversible process, but recent studies have shown that the committed cells can be reprogrammed into other lineage cells by modulating lineage-determining transcription factors (**Figure 2**) [6]. Transfection of CCAAT-enhancer-binding proteins (C/EBPs) transdifferentiates B cell progenitors into macrophages and other myeloid cells [7-9]. Similarly, deletion of Pax5 triggers dedifferentiation of mature B cells to early uncommitted progenitors, resulting in subsequent conversion into T cells or macrophages [10]. Overexpression of PU.1 alone or with C/EBPα causes reprogramming of T-committed precursors into dendritic cells or macrophages, respectively [11].

In several diseases, dysregulation of the lineage determinants also causes naturally occurring lineage conversion and contributes to pathogenesis (**Figure 3**). In relapsed leukemia patients, lineage switch between acute lymphoblastic leukemia (ALL) and acute myeloid leukemia (AML) is occasionally observed, allowing the abnormal bipotential leukemic clones to favorably survive against specific lineage-targeting immunotherapies [12]. Monocytic myeloid-derived suppressor cells (MDSCs) are reprogrammed into polymorphonuclear MDSCs by epigenetic silencing of *Rb1* in tumor-bearing mice and cancer patients. Moreover, I and my colleagues have

previously shown that the tumor microenvironment induces conversion of mature $CD11b^{+}CD27^{+}$ NK cells into MDSCs, and it can aggravate NK cell deficiency [13]. Although lineage conversions between immune cells have been reported in diseases and artificial culture systems, whether lineage reprogramming takes place and contributes immune cell development during homeostasis is poorly understood.

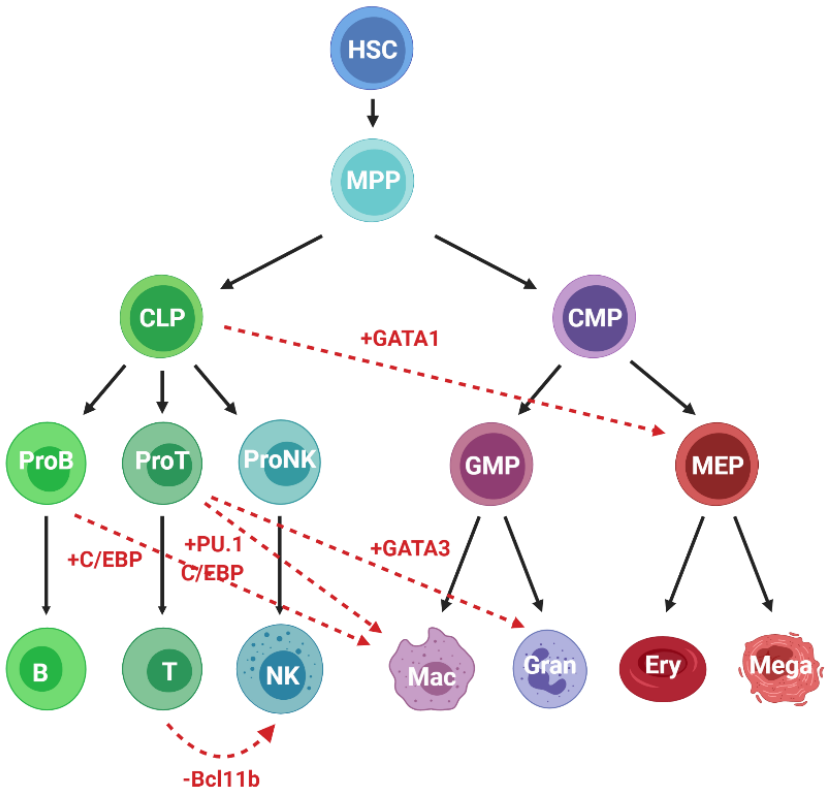

Figure 2. Aberrant expression of lineage determinants induces lineage reprogramming in hematopoiesis

The hematopoiesis is tightly regulated by a precise combination of lineage-specifying factors such as transcription factors and cytokines. However, it can be reprogrammed by manipulating the expression level of certain determinants. Solid lines indicate the normal lineage specifications, while dashed lines indicates altered lineage commitment. (Modified from Hu et al., Frontiers in Immunology 7, 268 (2017) [12])

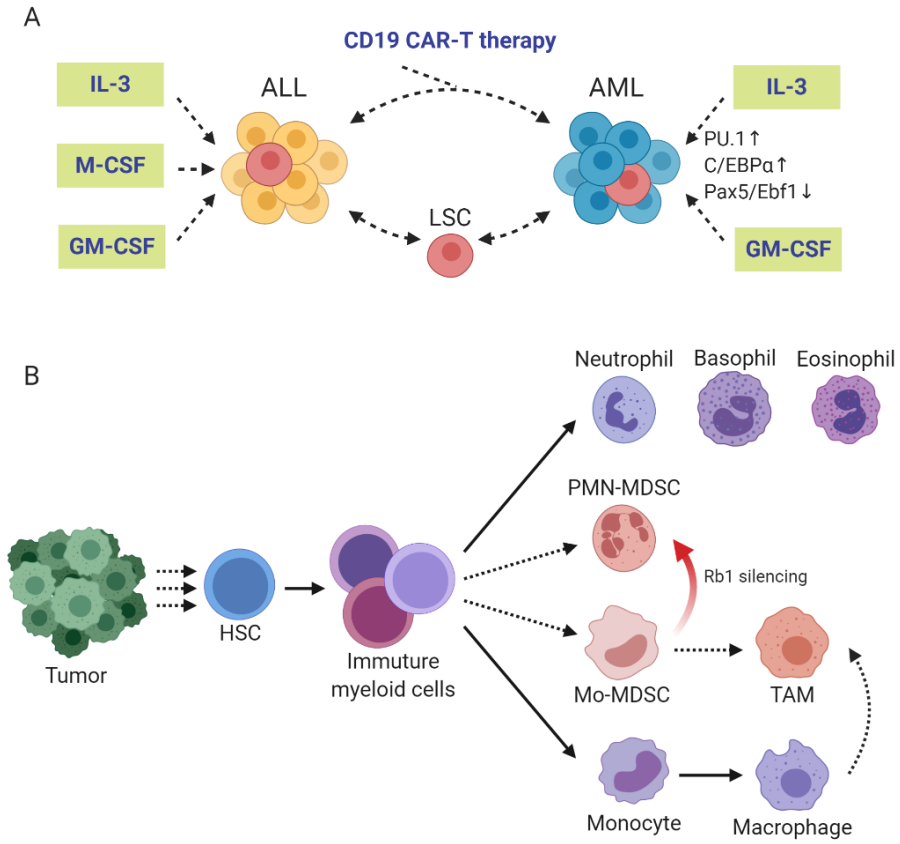

Figure 3. Natural occurring lineage conversion between immune cells

(**A**) In relapsed leukemia patients, lineage switch from acute lymphoblastic leukemia (ALL) to acute myeloid leukemia (AML) or *vice versa* are occasionally observed. The lineage switch could be mediated by therapy-mediated selection of bi-potential leukemic clones that can survive and expand during cancer therapy. (**B**) During tumor progression, a proportion of monocytic (M)-myeloid derived suppressor cells (MDSCs) were reprogrammed into polymorphonuclear (PMN)-MDSCs. This conversion is mediated by transcriptional silencing of the retinoblastoma gene through epigenetic modifications. Dashed lines indicate normal myeloid cell

development, while solid lines indicate abnormal myeloid cell development in tumor-bearing hosts. LSC, leukemia stem cell; TAM, tumor-associated macrophage (Modified from Hu et al., Frontiers in Immunology 7, 268 (2017) & Wynn, Nature Immunology 14, 197-199 (2013) [12,14])

III. Developmental relation between NK cells and myeloid cells

The developmental relationship between NK cells and myeloid cells is poorly understood. A clonal tracking study with hematopoietic stem/progenitor cell (HSPC) transplantation in humans revealed that NK cells from the bone marrow (BM) and peripheral blood cocluster with myeloid cells and independently group with T cells, suggesting a developmental proximity between NK cells and myeloid cells [15]. Indeed, human common myeloid progenitors (CMPs) and granulocyte-macrophage progenitors (GMPs) can develop into functional $CD56^{dim}$ NK cells in the presence of NK differentiation medium [16]. Moreover, GMP-derived $CD56^{+}CD33^{+}CD36^{+}$ cells have been found in human cord blood and BM and further differentiated into mature NK cells [17]. In *Csf2rb*$^{-/-}$ mice, ablation of GM-CSF signaling leads to a significant reduction in tissue-resident NK cells as well as myeloid cell populations [18].

IV. Purpose of this study

Although generation immunosuppressive neutrophils and monocytes from $CD11b^+CD27^+$ NK cells in tumor environment was revealed in the previous study, several issues were not resolved (**Figure 4**) [13]. Which can mark the myeloid-convertible NK cells and regulates the conversion remains to be clarified. Additionally, whether myeloid cells are developed from NK-committed cells during steady-state hematopoiesis has not yet been elucidated.

In the present study, I aimed to identify myeloid-convertible NK cells and key regulators of the NK cell conversion into myeloid cells. I demonstrated the conversion of NK cells into myeloid cells in naïve and tumor-bearing mice. A fate-tracing system revealed that $NKp46^+$ cells could contribute to myeloid cell development. Importantly, c-Kit^+CD24^+ cells among $CD11b^+CD27^+$ NK cells favorably differentiated into myeloid cell lineages *in vitro* and *in vivo*. Finally, transcriptome analysis and further experiments using chemical inhibitors showed GATA-2 was a molecular switch for this NK cell conversion. Collectively, I propose deep and novel insight for understanding the myeloid cell development.

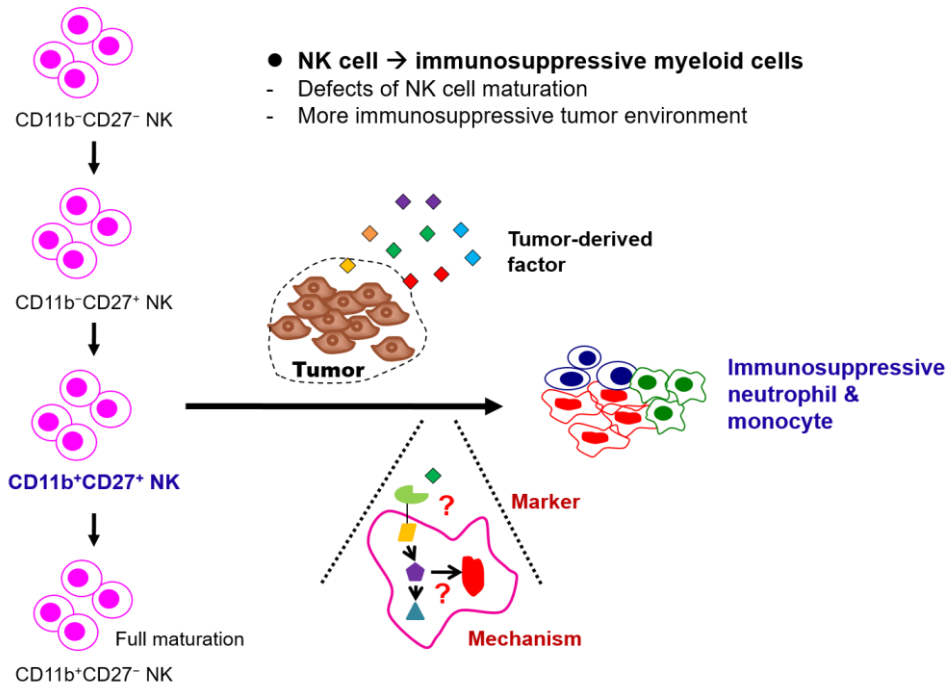

Figure 4. Lineage conversion of natural killer cells into myeloid-derived suppressor cells during tumor progression

A previous study from my laboratory showed tumor environment-mediated conversion of mature $CD11b^{+}CD27^{+}$ NK cells into immunosuppressive myeloid-derived suppressor cells in tumor-bearing mice, but cell surface markers and underlying mechanisms for the NK cell conversion were not defined. Whether the phenomenon also occurs in a steady state was not resolved in the previous study.

Materials and Methods

Mice

Female C57BL/6 and BALB/c mice were purchased from Charles River Laboratories (Seoul, Korea). *Ncr1*$^{iCRE/iCRE}$ and *R26R*$^{EYFP/EYFP}$ mice were kindly provided by Dr Eric Vivier (Aix-Marseille Université, Marseille, France). The *Ncr1*$^{iCRE/iCRE}$ and *R26R*$^{EYFP/EYFP}$ mice were crossed to obtain *Ncr*$^{iCRE/WT}$*R26R*$^{EYFP/WT}$ mice. Female C57BL/6 CD45.1^{+} congenic and OT-II mice were purchased from Jackson Laboratory (Bar Harbor, USA). The mice were bred and maintained in the specific pathogen-free animal facility at Seoul National University. Seven-to 10-week-old female mice were used in experiments. All animal experiments were approved by the Institutional Animal Care and Use Committee (IACUC; SNU-170504-4-3 & SNU-190516-1) of Seoul National University.

Cell lines and tumor model

The TC-1 lung carcinoma cells, YAC-1 lymphoma cells, and EL4 lymphoma cells were purchased from the American Type Culture Collection (ATCC). The cell lines were maintained in RPMI medium 1640 or Dulbecco's Modified Eagle Medium (Gibco, Gaithersburg, USA)

supplemented with 10% heat-inactivated FBS (Gibco) and 1% penicillin-streptomycin (Gibco). All cell lines were found to be negative for mycoplasma contamination. For the subcutaneous tumor model, 2×10^5 of the indicated tumor cells were subcutaneously injected into the left flank.

Flow cytometry and antibodies

Cells were stained with a cocktail of the specified antibodies in 50 or 100μL of buffer (PBS containing 1% FBS) with TruStain fcX (anti-mouse CD16/32) antibody (Clone 93, BioLegend, San Diego, USA). When two or more brilliant dyes were simultaneously used in samples, Brilliant Stain Buffer (BD Bioscience, San Jose, USA) was added to antibody cocktails. Intracellular staining for transcription factors or IFN-γ was performed after surface staining with the anti-mouse/rat Foxp3 staining set (eBioscience, San Diego, USA) or Cytofix/Cytoperm Fixation/Permeabilization kit (BD Bioscience), respectively. Cell apoptosis was measured by APC-conjugated Annexin V (BD Biosciences) and propidium iodide (PI, BD Biosciences) staining according to the manufacturer's recommendations. Dead cells were stained with Fixable Viability Dye (eBioscience) following the manufacturer's instruction. FACS-stained cells were acquired with a FACS Aria III or LSRFortessa X-20 instrument (BD Biosciences), and data were

analyzed using FlowJo software. The following anti-mouse antibodies were used: FITC-conjugated antibodies to CD24 (M1/69), CD27 (LG.3A10), IA/IE (M5/114.15.2), and Ly6C (HK1.4), PE-conjugated antibodies to 2B4 (m2B4(B6)458.1), c-Kit (2B8), CD4 (RM4-5), CD11c (N418), CD49a (HMα1), CD107a (1D4B), Eomes (Dan11mag, eBioscience), F4/80 (BM8), FcεRIα (MAR-1), GATA-3 (TWAJ, eBioscience), KLRG1 (2F1/KLRG1), Ly49A (A1(Ly49A), eBioscience), Ly49D (4E5), NKp46 (29A1.4), PDCA-1 (eBio129c, eBioscience), Siglec-F (E50-2440, BD Biosciences), T-bet (eBio4B10, eBioscience), and TRAIL (N2B2), PE-CF594-conjugated antibodies to CD11b (M1/70, BD Biosciences) and F4/80 (T45-2342, BD Biosciences), PerCP-Cy5.5-conjugated antibodies to CD3ε (145-2C11), CD19 (6D5), CD34 (HM34), Ly6G (1A8), IA/IE (M5/114.15.2), PE-Cy5-conjugated antibodies to CD19 (6D5) and c-Kit (2B8), PE-Cy7-conjugated antibodies to B220 (RA3-6B2), CD8α (53-6.7), CD122 (TM-β1), FcεRIα (MAR-1), Ly6G (1A8), and NK1.1 (PK136), APC-conjugated antibodies to B220 (RA3-6B2), CD3ε (145-2C11), CD11b (M1/70), CD11c (16A11), CD16/32 (93), CD24 (M1/69), CD25 (PC61), CD49b (DX5), CD127 (SB/199), F4/80 (BM8, eBioscience), FcεRIα (MAR-1), IFN-γ (XMG1.2), NK1.1(PK136), NKG2A (16A11), NKG2D (CX5), PBS-57-loaded CD1d tetramer (provided by National Institutes of Health (NIH) tetramer core

facility), and Sca-1 (E13-161.7), APC-R700-conjugated antibodies to CD11b (M1/70, BD Biosciences) and CD11c (N418, BD Biosciences), APC-eFluor780-conjugated antibodies to CD11b (M1/70, eBioscience), CD19 (eBio1D3, eBioscience), IA/IE (M5/114.15.2, eBioscience), and Ly6C (HK1.4, eBioscience), APC-Cy7-conjugated antibodies to CD27 (LG.3A10), Pacific Blue-conjugated antibodies to CD4 (RM4-5) and CD45.2 (104), BV421-conjugated antibodies to c-Kit (2B8, BD Biosciences), NKp46 (29A1.4, BD Biosciences), NK1.1(PK136, BD Biosciences), and RORγt (Q31-378, BD Biosciences), BV510-conjugated antibodies to CD24 (M1/69, BD Biosciences), BV786-conjugated antibodies to CD45.1 (A20, BD Biosciences), and BUV395-conjugated antibodies to NK1.1 (PK136, BD Biosciences). Antibodies were purchased from BioLegend unless otherwise indicated.

In vivo depletion of NK cells

Mice were intraperitoneally injected with 10 μL of anti-Asialo-GM1 antibody (BioLegend) or 100 μg rabbit serum IgG (Sigma Aldrich) three times every three days.

NK cell sorting

To enrich BM or splenic NK cells, depletion of CD3ε, CD19, and $Ly6G^+$ cells was followed by positive selection of $CD49b^+$ cells using magnetic microbeads (Miltenyi Biotec). For NK cell identification, at least two NK cell lineage markers ($CD122^+NK1.1^+$ for the C57BL/6 background or $CD122^+NKp46^+$ for the BALB/c background) were adopted. Specifically, Lin(CD3ε, CD19, CD34, and $Ly6G)^-CD122^+NK1.1$(or $NKp46)^+$ $CD11b^+CD27^+$ cells were gated for $CD11b^+CD27^+$ NK cells, and the $CD11b^+CD27^+$ NK cells were subsequently sorted based on c-Kit and/or CD24 expression by using the BD FACS Aria III.

NK cell culture

Sorted NK cells were suspended on 96-well U-bottom plates with the medium described below. RPMI medium 1640 (Gibco) supplemented with 10% heat-inactivated FBS (Gibco), penicillin-streptomycin (Gibco), MEM Non-Essential Amino Acids (Gibco), sodium pyruvate (Gibco), HEPES (Gibco), 2-Mercaptoethanol (Gibco). All cultures were incubated at 37℃ in a 5% CO_2 humidified atmosphere.

Reagents for NK cell culture

For differentiation of NK cells into myeloid cells, recombinant murine IL-3 (20 ng/ml, PeproTech, London, UK), recombinant murine IL-6 (20 ng/ml, PeproTech), recombinant murine SCF (50 ng/ml, R&D systems, Minneapolis, MN, USA) were used (M-medium). Recombinant murine IL-2 (PeproTech) or recombinant murine IL-15 (20 ng/ml, PeproTech) was added to block the differentiation. For inhibition of GATA-2 activity during the NK cell differentiation, K-7174 dihydrochloride (MedChemExpress) or mitoxantrone dihydrochloride (Sigma-Aldrich) was used.

Colony-forming unit assay

Mouse colony-forming unit assays were performed using Mouse Methylcellulose Complete Media (HSC007, R&D Systems) according to the manufacturer's protocol. Briefly, sorted NK cells (> 99.5% purity) were plated in methylcellulose medium at 10,000 cells per well. Colony formation was assessed after 10-14 days in culture by microscopy and scored on the basis of cellular morphology.

Cell imaging

Cultured cells were spun on slides with a cytospin centrifuge and stained with Diff-Quik (Sysmex, Kobe, Japan) according to the manufacturer's

instructions. Images of stained cells were acquired and analyzed with Vectra (PerkinElmer).

Phagocytosis assay

Phagocytosis assay was performed with pHrodo^{TM} Green *E. coli* Bioparticles conjugate (Invitrogen, Carlsbad, CA, USA) according to manufacturer's recommendations. After 1.5 hours of cell incubation, the cells were analyzed by flow cytometry.

***In vitro* T cell proliferation assay**

5×10^4 naïve $CD4^+$ T cells ($CD3\varepsilon^+CD4^+CD25^-CD62L^+CD44^-$ T cells from OT-II mice) and 1×10^4 myeloid cells or c-Kit^+CD24^+ NK cells (cultured or *ex vivo*) were co-cultured in the presence of ovalbumin peptide ($OVA_{323-339}$, 1 μg/ml). The $CD4^+$ T cells were labeled with 5 μM CellTrace Violet (Invitrogen) prior to co-incubation. After 4-5 days, the T cell proliferation and activation were determined by flow cytometry.

Adoptive cell transfer

For *in vivo* conversion of NK cells, $CD11b^{low/+}CD27^+$ NK cells were

obtained from the BM and spleens from naïve C57BL/6 mice. The 2×10^5 NK cells were transferred intravenously into CD45.1$^+$ recipient mice that were subcutaneously inoculated with 2×10^5 TC-1 tumor cells 10 days before the adoptive transfer. On day 2 or 6 after the NK cell transfer, CD45.2$^+$CD45.1$^-$ cells were analyzed for the phenotypes of NK cells and myeloid cells in the BM and spleen.

In vitro NK cell functional assay

To evaluate IFN-γ production and CD107a degranulation by NK cells, total BM and spleen cells were stimulated with cytokines (recombinant murine IL-12 (25 ng/ml) and recombinant murine IL-18 (20 ng/ml) or YAC-1 cells (1:5 ratio) for 4-5 hours in the presence of GolgiPlug (1 μg/ml, BD Biosciences) and 2.5 μg/ml anti-CD107a antibody. Following stimulation, intracellular IFN-γ staining was performed.

Transduction of lentiviral vector

Mouse GATA2 lentivirus (pLenti-GIII-CMV-GFP-2A-Puro) and its control (Lenti-CMV-GFP-2A-Puro-Blank lentivirus) were purchased from ABM (Milton, ON, Canada). Sorted NK cells were activated with IL-2 for 24

hours prior to viral infection. The activated NK cells were resuspended in viral supernatant (25 multiplicity of infection) in the presence of polybrene (8 μg/ml, Sigma Aldrich). Cell suspensions were placed in a 96-well culture plate and centrifuged at 2,000 rpm for 90 minutes at room temperature. Following infection, virus-containing supernatant was removed, and NK cells were restimulated in IL-2. After 6 hours, the medium was replaced with M-medium.

RNA sequencing and data processing

5,000 *ex vivo* NK cells from BALB/c BM (sorting purity > 99%) were lysed in TRIzol (Invitrogen). After 24 hours of M-medium treatment, live $CD122^{+}NKp46^{+}$ cells were directly collected into TRIzol and cell lysates from three independent experiments were mixed for one cDNA sample (~1,000 cells). Total RNAs were extracted from each sample using the TRIzol plus RNeasy micro kit (Qiagen). cDNA synthesis, library construction, RNA sequencing, and data processing were conducted at ChunLab (Seoul, Korea) and Macrogen (Seoul, Korea). The SMARTer Ultra Low Input RNA Kit (Clontech) was used for cDNA synthesis and amplification. NGS libraries were prepared with a TruSeq RNA Library Prep Kit (Illumina). Sequencing

was performed using an Illumina HiSeq2500 system with a 100-bp paired-end platform. Quality assessment for raw sequencing data was performed with FastQC v0.10.0. Raw reads were trimmed to eliminate low-quality reads, adaptor sequences, and poor-quality bases with Trimmomatic 0.32. The trimmed reads were mapped to a reference genome (UCSCmm10) with HISAT2 version 2.0.5. Transcript assembly was processed using reference-based aligned reads with StringTie version 1.3.3b. Gene expression values were normalized to FPKM (fragments per kilobase of transcript per million mapped reads). Differentially expressed genes (DEGs) were visualized using MeV version 4.9.0. Protein-protein interactions within the network were analyzed using the STRING database.

Quantitative real-time PCR

Total RNAs were extracted using the TRIzol reagent (Invitrogen) and reverse-transcribed using amfiRivert cDNA synthesis Platinum Master Mix (GenDEPOT). mRNA was quantified with a LightCycler optical system (Roche) and TB Green^{TM} Premix EX Taq Tli RNaseH Plus (Takara). The expression levels of target genes were calculated relative to *Hprt* expression. The following murine primers were used: *Gata2* forward: 5'-CAGGGAGACGATTGTGCTGA-3', *Gata2* reverse: 5'-

CTTCCGGTTAGGGTGCTCTG-3’, *Gfi1b* forward: 5’-

CCGCCTGCTTTAGTGTGTCT-3’, *Gfi1b* reverse: 5’-

CCCGAACTGACTCCCACATC-3’, *Lmo2* forward: 5’-

CTGAGGAACCCGTGGATGAG-3’, *Lmo2* reverse: 5’-

CGACACCCACAGAGGTCACA-3’, *Meis1* forward: 5’-

CGCCAGGGCTGCAAAGTAT-3’, *Meis1* reverse: 5’-

TGCACTCATTGTCGGGTCTC-3’, *Nfe2* forward: 5’-

GTTGTTGGCACAGTATCCGC-3’, *Nfe2* reverse: 5’-

CTCTTGCGACAGTTTTGGGC-3’, *Spi1* forward: 5’-

ATCTGGTGGGTGGAAAGGACAAA-3’, *Spi1* reverse: 5’-

GACTTTCTTCACCTCGCCTGTCTT-3’, *Id2* forward: 5’-

AGCATCCTGTCCTTGCAGGCATC-3’, *Id2* reverse: 5’-

CGTGTTCTCCTGGTGAAATGGCT-3’, *Ets1* forward: 5’-

TCATTTCTTTGCTGCTCGGA-3’, *Ets1* reverse: 5’-

AAGCCGACTCTCACCATCAT-3’, *Cebpa* forward: 5’-

CGGTGGACAAGAACAGCAAC-3’, *Cebpa* reverse: 5’-

ACGTTGCGTTGTTTGGCTTT-3’, *Cebpb* forward: 5’-

TGCAATCCGGATCAAACG-3’, *Cebpb* reverse: 5’-

AACCCCGCAGGAACATCTTT-3’, *Hprt* forward: 5’-

GGTGAAAAGGACCTCTCGAAGT-3', *Hprt* reverse: 5'-CAGGACTCCTCGTATTTGCAGA-3'

TNF ELISA

To evaluate TNF production, neutrophils were cultured at 1-2×10^6 cells/ml in the presence of LPS (1 μg/ml) and IFN-γ (50 ng/ml) for 24 hours. TNF concentration in the culture supernatant was determined using the mouse TNF ELISA set II (BD Bioscience) according to the manufacturer's instructions.

Statistics

Statistical comparisons were performed using GraphPad Prism 6 software. Data are represented as the means ± standard error of the mean (SEM). p-values were determined by the unpaired two-tailed Student's t test, unpaired two-tailed Mann-Whitney test, paired t test, or two-way ANOVA with Sidak's multiple comparisons test.

Data availability

The accession number for RNA sequencing data reported in this paper is GEO: GSE130250.

Results

NKp46^{+} cells contribute to myeloid cell development

To investigate the developmental contribution of NK cells to myeloid cells, I used *Ncr1*$^{iCRE/WT}$*R26R*$^{EYFP/WT}$ mice [19], in which NKp46-expressing cells and their progenies were irreversibly marked with EYFP expression by Cre recombinase (**Figure 5A**). Each immune cell population was gated as in **Table 1**. As expected, EYFP expression was found in nearly all NK cells and some iNKT cells, but a background frequency ranging from 0% to ~0.003% was found in HSPCs as well as T and B lymphocytes (**Figure 5B**). Given that tumors promote myelopoiesis and facilitate the differentiation of NK cells into immunosuppressive myeloid cells [13], I examined whether tumors trigger the differentiation of NK cells into myeloid cells in this system. *Ncr1*$^{iCRE/WT}$*R26R*$^{EYFP/WT}$ mice were subcutaneously injected with TC-1 tumor cells, and NKp46^{+} cell-derived myeloid cells were analyzed at day 14, when tumor-associated neutrophils, also termed polymorphonuclear MDSCs, had sufficiently accumulated in the spleen (**Figure 6A**). The EYFP^{+} tumor-associated myeloid cells were found in lymphoid organs and tumor tissues from TC-1 tumor-bearing mice (**Figure 6B**). Additionally, these cell

populations were also detected in the spleen from EL4 solid tumor-bearing mice (**Figure 6C**).

Next, when examining their contribution to myeloid cell development in naïve *Ncr1*$^{iCRE/WT}$*R26R*$^{EYFP/WT}$ mice, EYFP expression was observed in a few cells among most myeloid lineages expressing specific myeloid cell markers with large cell sizes and high granularities (**Figure 7A**). However, the majority of EYFP$^+$ myeloid cells still expressed NK cell markers (**Figure 7B**). However, the frequencies and numbers of EYFP$^+$ myeloid cells were low in lymphoid organs from naïve mice (**Figure 7C, D**). When I compared the frequencies and numbers of EYFP$^+$ myeloid cells in naïve and tumor-bearing mice, the number of EYFP$^+$ neutrophils was increased in the spleen from TC-1 tumor-bearing mice due to tumor-promoting accumulation of myeloid cells. However, the frequencies and numbers of EYFP$^+$ myeloid cells in most organs from tumor-bearing mice were similar to those from naïve mice (**Figure 6D**).

In addition, when I examined whether the EYFP$^+$ myeloid cells are functional, EYFP$^+$ neutrophils showed similar or less TNF secretion in response to LPS and IFN-γ stimulation, compared to EYFP$^-$ neutrophils (**Figure 8A**). Similarly, EYFP$^+$ Mono/moDCs activated ovalbumin-specific CD4$^+$ T cells to a similar extent as EYFP$^-$ Mono/moDCs (**Figure 8B**).

Furthermore, the functions of $EYFP^+$ neutrophils and monocytes from the tumor-bearing mice were slightly increased compared to naïve mice, but the difference was not significant (**Figure 8**).

To demonstrate whether the $EYFP^+$ myeloid cells are NK cell-derived, NK cells were depleted through anti-Asialo-GM1 antibody administration. As a result, $EYFP^+$ myeloid cell populations were almost eliminated without a loss of $EYFP^-$ myeloid cells in lymphoid organs from anti-Asialo-GM1-treated mice, indicating that the $EYFP^+$ myeloid cells were derived from NK cells (**Figure 9**). The presence of $EYFP^+$ myeloid cells suggests the possibility that NK-phenotype cells differentiate into myeloid cells under steady-state conditions and in a tumor environment.

Table 1. Surface marker phenotypes to define immune cells from *Ncr1*$^{iCRE/WT}$*R26R*$^{EYFP/WT}$ mice

Population	Surface phenotype
NK	CD3ε$^-$CD19$^-$CD4$^-$CD8$^-$CD1d-Tetramer$^-$NK1.1$^+$
iNKT	CD3ε$^+$ CD1d-Tetramer$^+$CD19$^-$CD8$^-$
CD4 T	CD3ε$^+$CD19$^-$CD1d-Tetramer$^-$NK1.1$^-$CD4$^+$CD8$^-$
CD8 T	CD3ε$^+$CD19$^-$CD1d-Tetramer$^-$NK1.1$^-$CD4$^-$CD8$^+$
B	CD3ε$^-$ CD1d-Tetramer$^-$NK1.1$^-$CD4$^-$CD8$^-$CD19$^+$
LT-HSC	Lineage$^-$Sca-1$^+$c-Kit$^+$FLT3$^-$CD34$^-$
ST-HSC	Lineage$^-$Sca-1$^+$c-Kit$^+$FLT3$^-$CD34$^+$
MPP	Lineage$^-$Sca-1$^+$c-Kit$^+$FLT3$^+$CD34$^+$
CLP	Lineage$^-$Sca-1$^-$c-Kit$^+$CD127$^+$
CMP	Lineage$^-$Sca-1$^-$c-Kit$^+$ CD127$^-$CD16/32$^-$CD34$^+$
GMP	Lineage$^-$Sca-1$^-$c-Kit$^+$ CD127$^-$CD16/32$^+$CD34$^+$
MEP	Lineage$^-$Sca-1$^-$c-Kit$^+$ CD127$^-$CD16/32$^-$CD34$^-$
Neutrophil	CD11b^{high}Ly6C$^{-/low}$Ly6G$^+$
Monocyte	CD11b^{high}Ly6G$^-$Ly6C^{high}IA/IE$^-$
Macrophage	CD11b^{high}Ly6G$^-$Ly6C$^{-/low}$IA/IE$^+$F4/80$^+$
moDC	CD11b^{high}Ly6G$^-$Ly6C$^{int/high}$IA/IE$^+$
cDC	CD11c^{high}IA/IE^{high}B220$^-$PDCA-1$^-$
pDC	PDCA-1$^+$B220$^+$CD11b$^-$CD11c$^+$
Eosinophil	CD3ε$^-$CD19$^-$CD11b$^+$Siglec-F$^+$SSC^{high}
Basophil	CD3ε$^-$CD19$^-$Siglec-F$^-$c-Kit$^-$FcεRIα$^+$

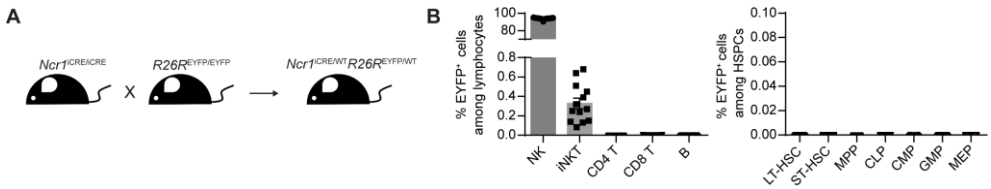

Figure 5. Lineage tracing of NKp46^{+} cells in *Ncr1*$^{\mathbf{iCRE/WT}}$*R26R*$^{\mathbf{EYFP/WT}}$ mice

(**A**) Schematic representation of *Ncr1*$^{iCRE/WT}$*R26R*$^{EYFP/WT}$ mice. The *Ncr1*$^{iCRE/iCRE}$ mice were crossed to *R26R*$^{EYFP/EYFP}$ mice to generate *Ncr1*$^{iCRE/WT}$*R26R*$^{EYFP/WT}$ mice, in which NKp46-expressing cells and their progenies were irreversibly labeled with EYFP (C57BL/6 background). (**B**) The frequency of EYFP^{+} cells in splenic lymphocytes and BM HSPCs from naïve *Ncr1*$^{iCRE/WT}$*R26R*$^{EYFP/WT}$ mice. Data represent two independent experiments.

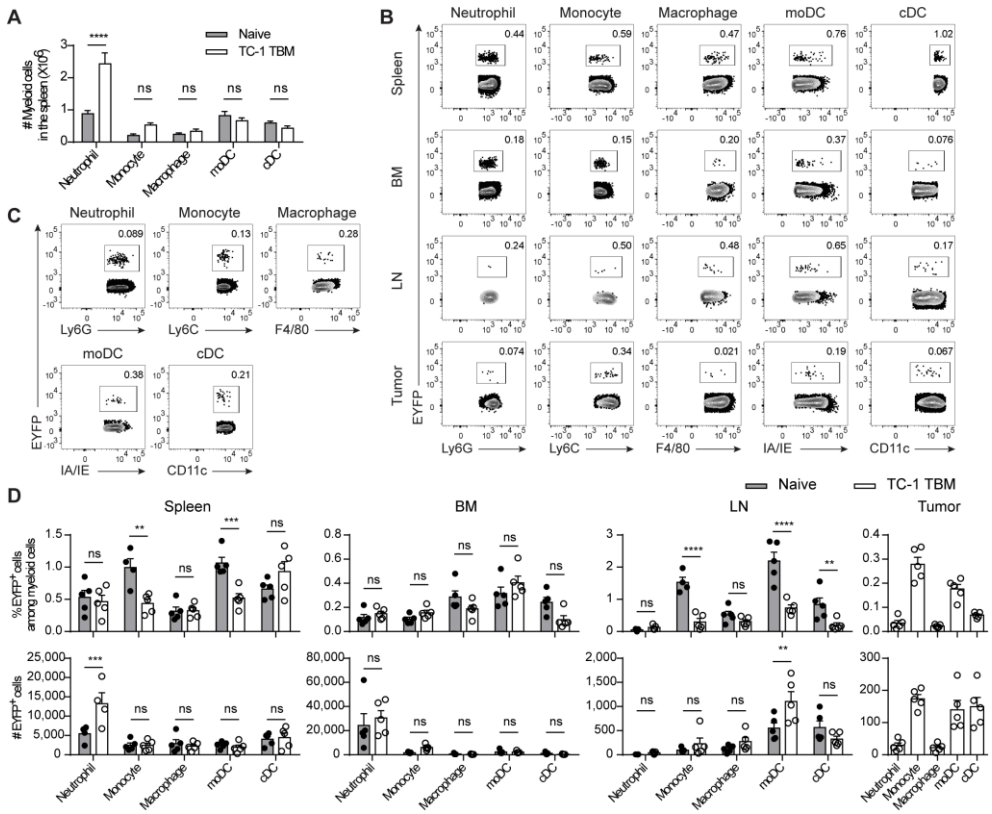

Figure 6. The number of NKp46^{+} cell-derived neutrophils is increased in the spleen from TC-1 tumor-bearing mice

(**A**) Quantification of myeloid cells in the spleen from naïve and 2-week TC-1 tumor-bearing *Ncr1*$^{\text{iCRE/WT}}$*R26R*$^{\text{EYFP/WT}}$ mice. (**B**) Representative results for EYFP expression on myeloid cell populations in lymphoid organs and tumors from 2-week TC-1 tumor-bearing *Ncr1*$^{\text{iCRE/WT}}$*R26R*$^{\text{EYFP/WT}}$ mice. (**C**) Flow-cytometric analysis of EYFP expression on splenic myeloid cell populations from 2.5-week EL4 tumor-bearing *Ncr1*$^{\text{iCRE/WT}}$*R26R*$^{\text{EYFP/WT}}$ mice. (**D**) The frequency and number of EYFP^{+} cells in the indicated cell populations in

naïve or 2-week TC-1 tumor-bearing *Ncr1*$^{iCRE/WT}$*R26R*$^{EYFP/WT}$ mice. The number of tumor-infiltrating myeloid cells per gram of tumor was quantified. (**A**−**D**) After doublet discrimination, each immune cell population was gated as in Table 1. Data represent three independent experiments. ** p-value<0.01, *** p-value<0.001, **** p-value<0.0001 by two-way ANOVA.

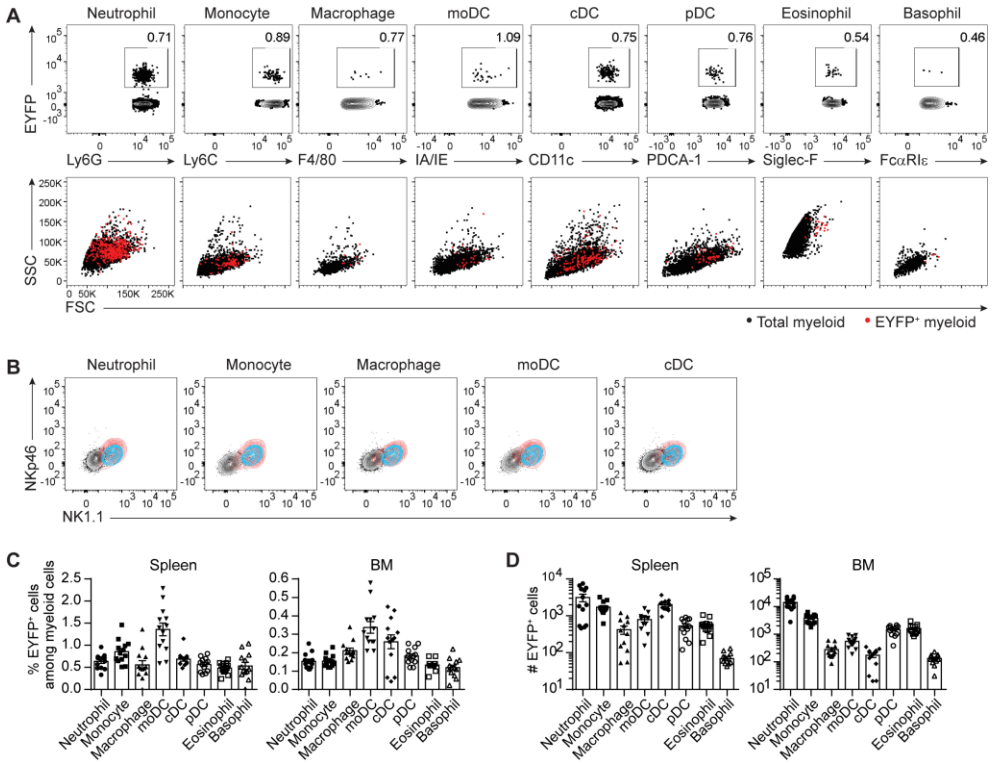

Figure 7. Lineage tracing of NKp46^{+} cells provides evidence for NK-derived myeloid cell populations in a steady state

(**A**) Flow-cytometric analysis of EYFP expression (upper panel) and forward and side scatter intensity (low panel) on myeloid cells in the spleen from naïve *Ncr1*$^{iCRE/WT}$*R26R*$^{EYFP/WT}$ mice. Total myeloid cells and EYFP^{+} myeloid cells are plotted in black and red, respectively. (**B**) Representative results of NK cell marker expression on the indicated splenic myeloid cell population. Total myeloid cells, EYFP^{+} myeloid, and NK cells are plotted in black, red, and blue, respectively. (**C**, **D**) The frequency and number of EYFP^{+} cells in the

myeloid cell populations (BM: tibias and femurs from both legs), and data were pooled from two independent experiments (n=7 and n=6, respectively). (**A**−**D**) After doublet discrimination, each immune cell population was gated as in Table 1. Data represent at least four independent experiments.

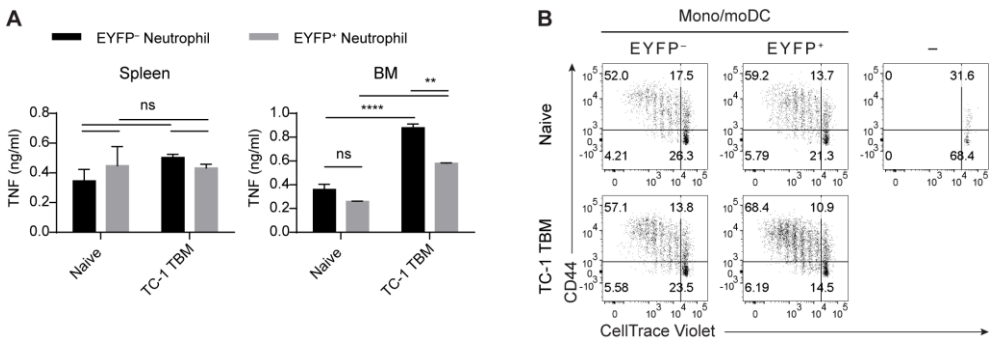

Figure 8. NK-derived EYFP$^+$ myeloid cells have functions similar to those of conventional myeloid cells

(**A**) TNF secretion by EYFP$^-$ or EYFP$^+$ neutrophils (CD11b$^+$Ly6G$^+$Ly6C$^-$) in response to LPS and IFN-γ stimulation for 24 hours. (**B**) Proliferation and activation of OT-II-derived naïve CD4$^+$ T cells in the presence of EYFP$^-$ or EYFP$^+$ Mono/moDCs (CD11b$^+$Ly6G$^-$Ly6C$^+$IA/IE$^{-/+}$) after co-incubation for 5 days. ** p-value<0.01, **** p-value<0.0001 by two-way ANOVA.

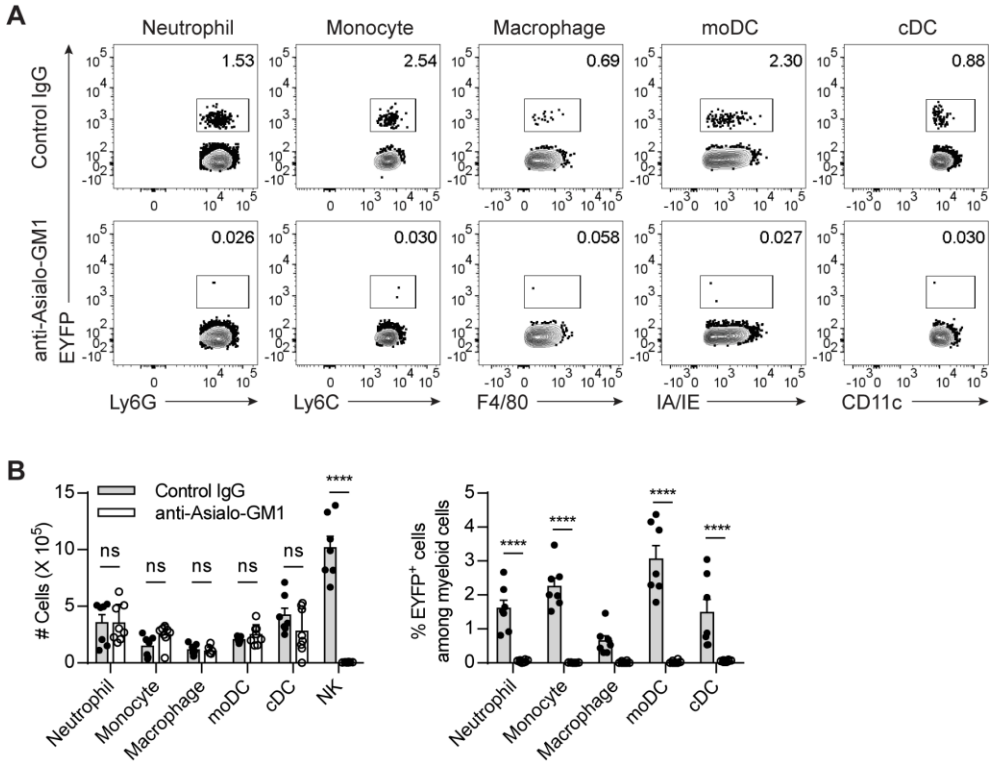

Figure 9. NK cell-depleting anti-Asialo-GM1 selectively ablate EYFP$^+$ myeloid cells *in vivo*

(**A**) Flow-cytometric analysis of EYFP expression on myeloid cells in the spleen from *Ncr1*$^{iCRE/WT}$*R26R*$^{EYFP/WT}$ mice that received an intraperitoneal injection of anti-Asialo-GM1 or control IgG to deplete NK cells. (**B**) The number of EYFP$^-$ myeloid cells and frequency of EYFP$^+$ myeloid cells in the spleen from anti-Asialo-GM1-treated *Ncr1*$^{iCRE/WT}$*R26R*$^{EYFP/WT}$ mice. Data represent two independent experiments. **** p-value<0.0001 by two-way ANOVA.

c-Kit$^+$CD24$^+$CD11b$^+$CD27$^+$ NK cells are reprogrammed into myeloid cells *in vitro*

CD11b$^+$CD27$^+$ NK cells were predominantly converted into CD11b$^+$Gr-1$^+$ myeloid cells [13]. c-Kit expression is found in CD11b$^{-/+}$CD27$^+$ NK cells but is lost upon final maturation into CD11b$^+$CD27$^-$ NK cells [20]. Additionally, c-Kit is mainly expressed on HSPCs and regulates their stem cell properties, such as self-renewal and differentiation [21,22]. Thus, I evaluated whether c-Kit is a potential marker for the differentiation of CD11b$^+$CD27$^+$ NK cells into myeloid cells. I separately sorted CD11b$^+$CD27$^+$ NK cells, hereafter termed NK cells, based on c-Kit expression (**Figure 10A, B**) and then cultured them in medium containing IL-3, IL-6, and SCF for myeloid cell development (M-medium) [23,24]. c-Kit$^-$ NK cells did not survive due to the absence of NK-supporting stimuli, but c-Kit$^+$ NK cells differentiated into myeloid cells (**Figure 11**), indicating that c-Kit could mark the NK cells with myeloid developmental potentiality.

To identify additional markers for myeloid-producible NK cells, I comparatively analyzed transcriptome profiles between c-Kit$^-$ and c-Kit$^+$ NK cells. None of the analyzed c-Kit$^-$ or c-Kit$^+$ NK cell samples showed expression of representative genes defining other lineage immune cells (**Figure 12A**). Among DEGs with products expressed on the plasma

membrane, I focused on *Cd24a*, encoding CD24, a marker of pluripotent cells (**Figure 12B**) [25,26]. CD24 was substantially upregulated in c-Kit$^+$ NK cells from lymphoid organs (**Figure 12C**). I also found that CD24 was consistently expressed during all maturation stages of BM NK cells (**Figure 12D**).

To determine whether CD24 is an additional marker for the NK cell differentiation, highly pure c-Kit$^+$CD24$^+$ NK cells were obtained (**Figure 10A, C**) and then cultured in the M-medium. As a result, c-Kit$^+$CD24$^+$ NK cells differentiated into granulocytes and monocytes/macrophages (**Figure 13A**). However, the other three CD11b$^+$CD27$^+$ NK populations and c-Kit$^+$CD24$^+$ cells in immature CD11b$^-$CD27$^+$ NK cells underwent apoptosis instead of differentiation under M-medium culture (**Figure 13B**). To confirm myeloid cell development from c-Kit$^+$CD24$^+$ NK cells in another culture system, I sorted NK cells based on c-Kit and CD24 expression and cultured them in methylcellulose medium supporting myeloid cell differentiation to perform a colony-forming unit assay. Notably, colonies were only observed in c-Kit$^+$CD24$^+$ NK cell cultures, and included erythrocyte/megakaryocyte-containing colonies as well as myeloid cell colonies (**Figure 14A, B**). The conversion efficiency for c-Kit$^+$CD24$^+$ NK cells was low, but the other NK cell subsets and lymphocytes could not generate myeloid cells at all (**Figure 14**).

To clearly examine if the myeloid cells originated from NK cells, EYFP$^+$c-Kit$^+$CD24$^+$ NK cells isolated from *Ncr1*$^{iCRE/WT}$*R26R*$^{EYFP/WT}$ mice were sorted and cultured in M-medium for 7 days. Myeloid cells differentiated from EYFP$^+$c-Kit$^+$CD24$^+$ NK cells maintained EYFP expression (**Figure 15A**), indicating the development of myeloid cells from c-Kit$^+$CD24$^+$ NK cells. I also included other myeloid-specific markers to clearly assess the myeloid cell phenotype of cells produced from c-Kit$^+$CD24$^+$ NK cells during M-medium culture. As expected, CD11b$^+$ progenies included CD115$^-$ neutrophils and CD115$^+$ monocyte-derived cells (monocytes, moDCs, and macrophages), while some of CD11b$^{-/low}$ progenies were FcεRIα$^+$ basophils/mast cells (**Figure 15B**). Furthermore, c-Kit$^+$CD24$^+$ NK cells gradually acquired the expression of myeloid cell markers such as CD11b, Ly6C, and Ly6G and lost their NK 1.1 expression during the conversion into myeloid cells, which enabled the detection of the intermediate cell population with an NK-myeloid mixed phenotype (**Figure 15C**). When I tested the minimum cytokine requirements for the myeloid cell development from c-Kit$^+$CD24$^+$ NK cells, IL-3 was an indispensable cytokine in M-medium, albeit it was ineffective on its own (**Figure 15D**).

In addition, I examined whether stimulated c-Kit$^+$CD24$^+$ NK cells also differentiate into myeloid cells. Sorted c-Kit$^+$CD24$^+$ NK cells were

prestimulated with a combination of IL-2 and αNK1.1 antibody, IL-12, IL-18, or IL-21 for 48 hours, and the activated NK cells were recultured with M-medium for 6 days. As a result, I found that c-Kit^{+}CD24^{+} NK cells were capable of myeloid cell development regardless of the activation status (**Figure 16**). Furthermore, c-Kit^{+}CD24^{+} NK cells were primarily distributed in lymphoid organs, and c-Kit^{+}CD24^{+} NK cells derived from the BM and spleen limitedly differentiated into myeloid cells (**Figure 17**).

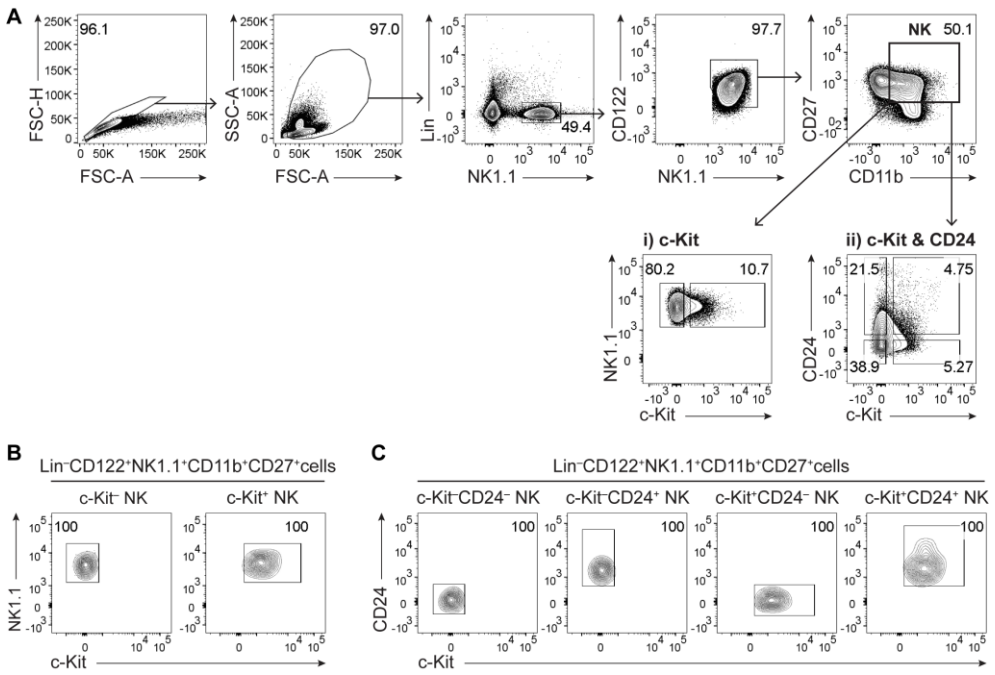

Figure 10. Gating strategy for NK cell sorting

(**A**) C57BL/6 BM CD3ε/CD19/Ly6G-expressing cells were depleted, and then CD49b-positive cells were enriched by MACS. During FACS sorting, cell aggregates and debris were gated out. $CD11b^+CD27^+$ NK cells were gated as Lin $(CD3\varepsilon/CD19/CD34/Ly6G)^-NK1.1^+CD122^+CD11b^+CD27^+$ cells. In my study, $CD11b^+CD27^+$ NK cells are referred to simply as NK cells for convenience. $CD11b^+CD27^+$ NK cells were further divided based on c-Kit and/or CD24 expression. The overall phenotype of c-Kit^-, c-Kit^+, c-Kit^-CD24^-, or c-Kit^+CD24^+ NK cells is $Lin^-CD122^+NK1.1^+CD11b^+CD27^+$ c-Kit^-, $Lin^-CD122^+NK1.1^+CD11b^+CD27^+$c-$Kit^+$, $Lin^-CD122^+NK1.1^+$

$CD11b^{+}CD27^{+}c\text{-}Kit^{-}CD24^{-}$, or $Lin^{-}CD122^{+}NK1.1^{+}CD11b^{+}CD27^{+}c\text{-}Kit^{+}$ $CD24^{+}$ cells, respectively. (**B, C**) Re-analysis profiles of sorted $c\text{-}Kit^{-}$ or $c\text{-}Kit^{+}$ NK cells (**B**) and $c\text{-}Kit^{-}CD24^{-}$, $c\text{-}Kit^{-}CD24^{+}$, $c\text{-}Kit^{+}CD24^{-}$, or $c\text{-}Kit^{+}CD24^{+}$ NK cells (**C**) from C57BL/6 BM.

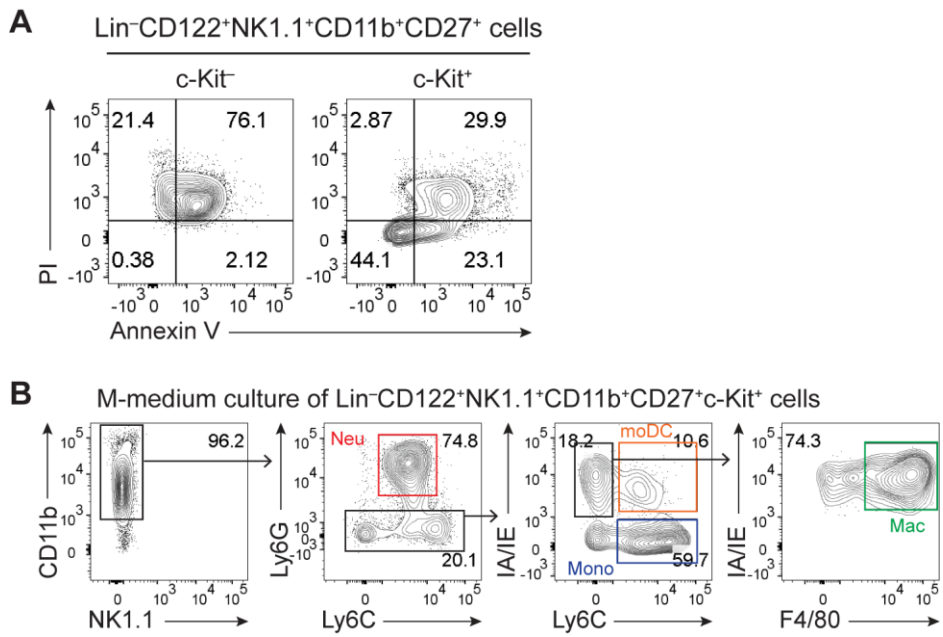

Figure 11. c-Kit marks CD11b$^+$CD27$^+$ NK cells with the potential for myeloid cell development

(**A**) NK cells (Lin$^-$CD122$^+$NK1.1$^+$CD11b$^+$CD27$^+$ cells) from C57BL/6 BM were sorted based on c-Kit expression. The sorted BM NK cells were cultured in M-medium for 5 days, and cell apoptosis was determined by Annexin V and PI staining. (**B**) C57BL/6 BM-derived c-Kit$^+$ NK cells were cultured in M-medium (containing IL-3, IL-6, and SCF) for 7 days, and then myeloid cell phenotypes were assessed by flow cytometry. The whole phenotype of sorted c-Kit$^+$ NK cells is Lin(CD3ε/CD19/CD34/Ly6G)$^-$CD122$^+$NK1.1$^+$CD11b$^+$ CD27$^+$c-Kit$^+$. Data represent two (A) or at least five (B) independent experiments.

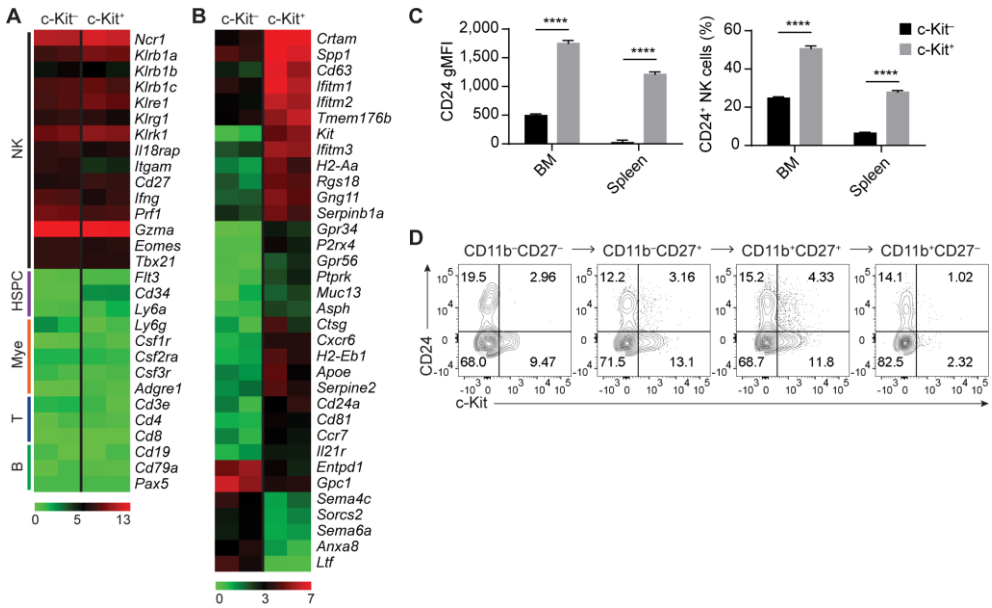

Figure 12. CD24 is upregulated in c-Kit$^+$CD11b$^+$CD27$^+$ NK cells

(**A**) Transcriptome profiles for hematopoietic cell lineage-related genes. (**B**) Transcriptome analysis of genes that were significantly upregulated or downregulated by at least 5.0-fold in c-Kit$^+$ NK cells relative to their expression in c-Kit$^-$ NK cells. The heatmap of DEGs encoding plasma membrane proteins is indicated. (**A**, **B**) The color scale represents the log2 (FPKM+1). (**C**) Geometric mean fluorescence intensity and frequency of CD24 expression in BALB/c-derived NK cells. (**D**) Expression of c-Kit and CD24 in C57BL/6 BM NK cells during NK cell maturation. Data represent at least five independent experiments (C, D). **** p-value<0.0001 by two-way ANOVA.

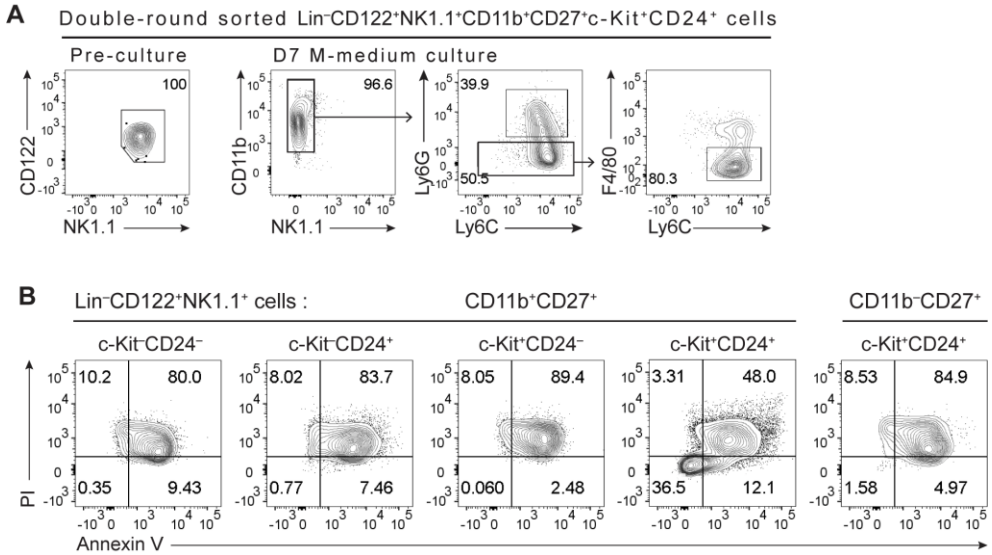

Figure 13. c-Kit$^+$CD24$^+$ NK cells predominantly differentiate into myeloid lineages *in vitro*

(**A**) C57BL/6 BM-derived c-Kit$^+$CD24$^+$ NK cells highly purely obtained through double-round sorting were cultured in M-medium. After 7 days, myeloid cell phenotypes were assessed by flow cytometry. The whole phenotype of sorted c-Kit$^+$CD24$^+$ NK cells is Lin(CD3ε/CD19/CD34/Ly6G)$^-$ CD122$^+$NK1.1$^+$CD11b$^+$CD27$^+$c-Kit$^+$CD24$^+$. (**B**) NK cells (Lin$^-$CD122$^+$ NK1.1$^+$CD11b$^+$CD27$^+$ cells) from C57BL/6 BM were sorted based on c-Kit/CD24 expression. The sorted BM NK cells were cultured in M-medium for 5 days, and cell apoptosis was determined by Annexin V and PI staining. Data represent three (A) or two (B) independent experiments.

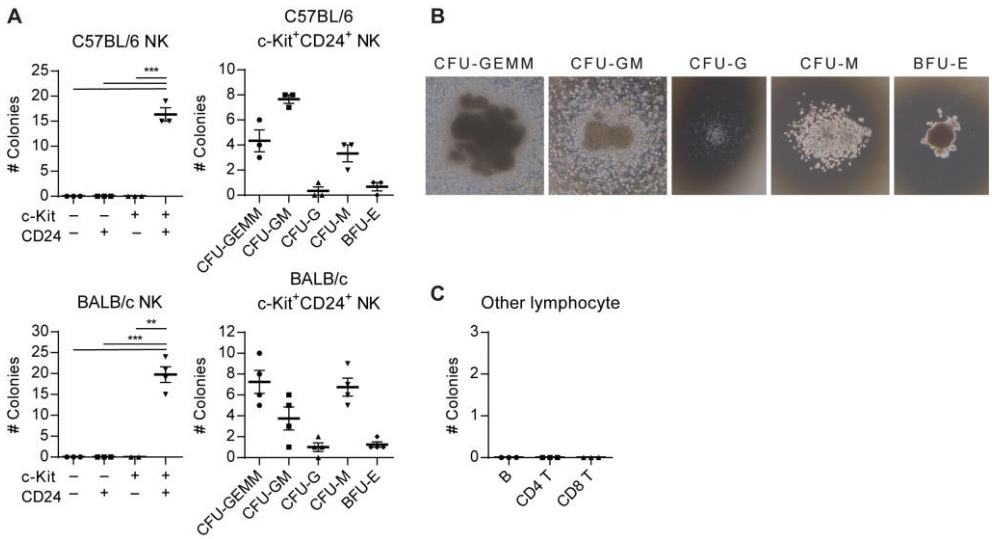

Figure 14. Colony-forming unit assay shows that c-Kit$^+$CD24$^+$ NK cells differentiate into myeloid lineage cells

(**A**) BM NK cells from naïve mice (upper: C57BL/6, lower: BALB/c) were purely sorted and cultured in methylcellulose complete medium for myeloid development (10,000 cells per well). Cell colonies were identified and scored at 12 days, and colony types included CFU-GEMM (colony-forming unit-granulocyte, erythrocyte, macrophage, megakaryocyte), CFU-GM (colony-forming unit-granulocyte, macrophage), CFU-G (colony-forming unit-granulocyte), CFU-M (colony-forming unit-macrophage), and BFU-E (burst-forming unit-erythroid). (**B**) Photographs of each cell colony from the (**A**) upper panel−C57BL/6 c-Kit$^+$CD24$^+$ NK cells at a magnification of 40X. (**C**) The ability of B or T lymphocytes from naïve C57BL/6 BM to form myeloid

cell colonies (10,000 cells per well). ** p-value<0.01, *** p-value<0.001 by the Student's t test. Data represent at least four (A, B) or two (C) independent experiments.

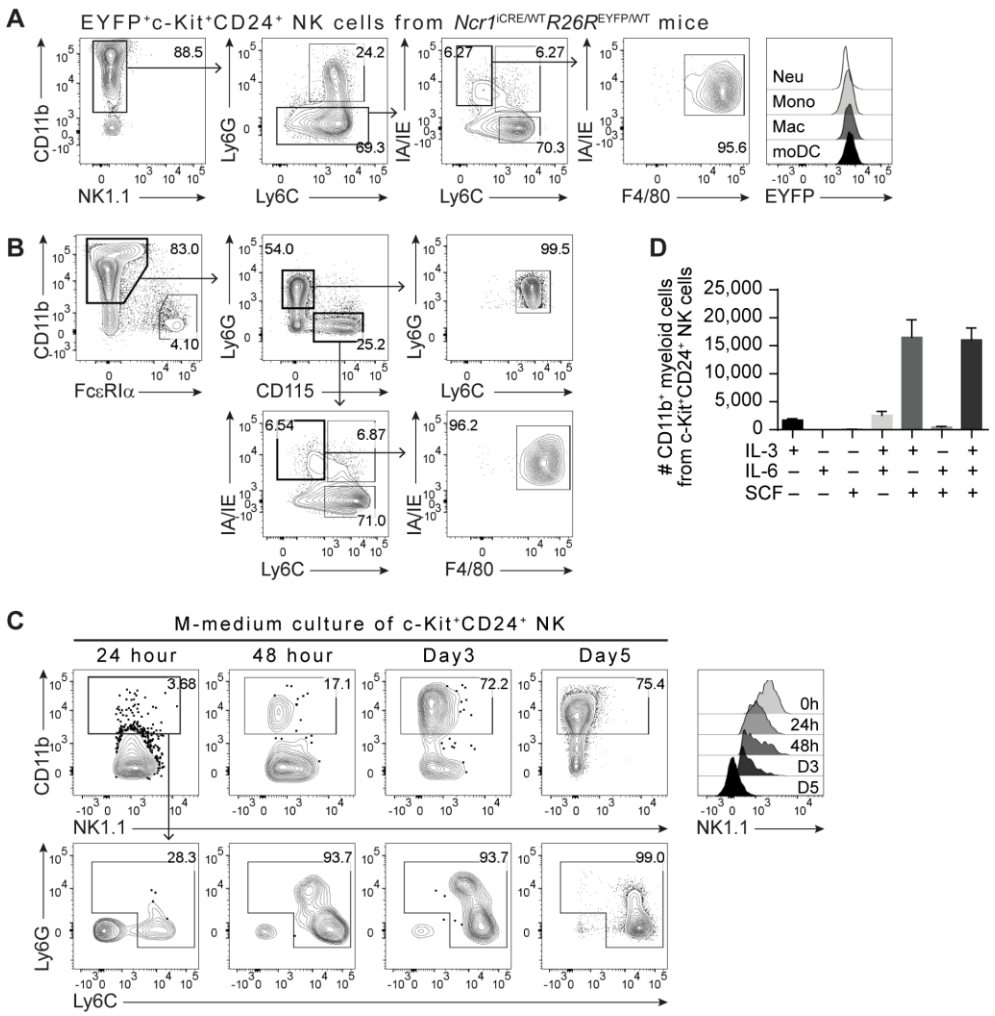

Figure 15. c-Kit$^+$CD24$^+$ NK cells acquire expression of myeloid cell markers with loss of NK cell phenotype during the conversion into myeloid cells

(**A**) EYFP$^+$c-Kit$^+$CD24$^+$ NK cells from *Ncr1*$^{iCRE/WT}$*R26R*$^{EYFP/WT}$ mice were cultured in M-medium for 7 days. The production of EYFP$^+$ myeloid cells was analyzed in EYFP$^+$ progenies through flow cytometry. (**B**) C57BL/6 BM-

derived c-Kit$^+$ NK cells were cultured in M-medium for 7 days, and then myeloid cell phenotypes were assessed by flow cytometry. (**C**) Flow cytometric analysis showing the acquisition of the myeloid phenotypes and loss of NK1.1 expression (gMFI) in live CD11b$^+$ cells at various time points following M-medium culture of C57BL/6 BM-derived c-Kit$^+$CD24$^+$ NK cells. (**D**) C57BL/6 BM-derived c-Kit$^+$CD24$^+$ NK cells were cultured in the presence of combinations of M-medium-containing cytokines. After 7 days, the number of CD11b$^+$Gr-1$^+$ myeloid cells (containing neutrophils, monocytes, and macrophages) was quantified. Data represent two (A) or three (B−D) independent experiments.

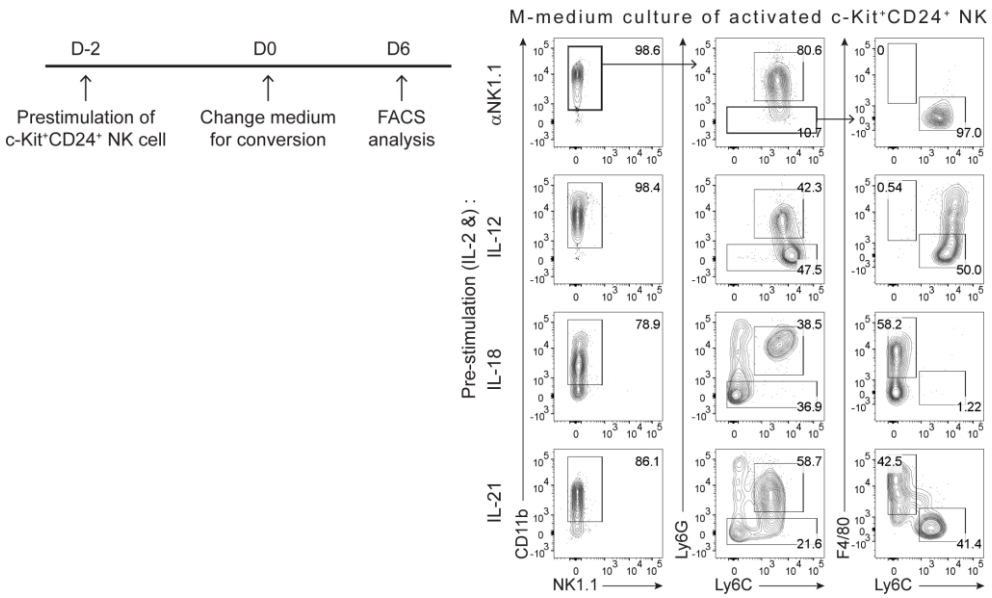

Figure 16. Activated c-Kit$^+$CD24$^+$ NK cells also differentiate into myeloid cells

Sorted C57BL/6 BM c-Kit$^+$CD24$^+$ NK cells were prestimulated for 48 hours with a combination of IL-2 (5 ng/ml) and coated αNK1.1 antibody (25 μg/ml), IL-12 (20 ng/ml), IL-18 (20 ng/ml), or IL-21 (20 ng/ml). After cell washing, activated NK cells were subsequently recultured in M-medium for 6 days, and converted cells were analyzed by flow cytometry. Data represent three independent experiments.

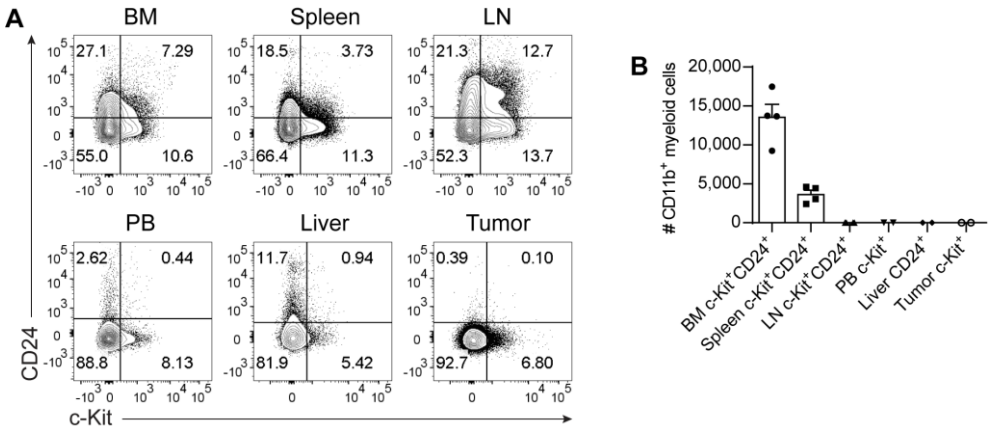

Figure 17. The differentiation of c-Kit$^+$CD24$^+$ NK cells into myeloid cells occurs depending on tissue origin of the NK cells

(**A**) Flow-cytometric analysis of c-Kit and CD24 expression on NK cells derived from lymphoid organs and tissues from C57BL/6 mice. NK cells were identified by Lin(CD3/CD19/CD34/Ly6G)$^-$CD122$^+$NK1.1$^+$CD11b$^+$CD27$^+$ (BM, spleen, axillary/bronchial/inguinal lymph nodes, and peripheral blood) or Lin$^-$NK1.1$^+$CD49b$^+$CD49a$^-$CD11b$^+$CD27$^+$ (perfused liver and TC-1 tumor tissue) phenotype. (**B**) C57BL/6 NK cells were cultured in M-medium. After 7 days, the number of CD11b$^+$ myeloid cells (neutrophil, monocytes, moDCs, and macrophages) were quantified (4×10^4 cells per well for BM or splenic NK cells, $1\text{-}2\times10^4$ cells per well for LN, liver, and TC-1 tumor-infiltrating NK cells). Data represent three independent experiments.

NK-stimulatory cytokines inhibit the myeloid cell development from c-Kit$^+$CD24$^+$ NK cells

My colleague and I have previously shown that the NK-stimulatory cytokines (IL-2 and IL-15) inhibit the differentiation of NK cells into immunosuppressive myeloid cells in the tumor microenvironment [13]. Thus, I tested whether the NK-stimulating cytokines also block the differentiation of c-Kit$^+$CD24$^+$ NK cells into myeloid cells. Although myeloid cell development from hematopoietic stem and multipotent progenitor cells (Lin$^-$Sca-1$^+$c-Kit$^+$CD34$^+$ LSK) and myeloid progenitors (Lin$^-$Sca-1$^-$c-Kit$^+$CD34$^+$CD16/32$^-$ CMP and Lin$^-$Sca-1$^-$c-Kit$^+$CD34$^+$CD16/32$^+$ GMP) were not affected in the presence of IL-2 or IL-15, these two cytokines almost completely inhibited myeloid cell production of c-Kit$^+$CD24$^+$ NK cells and maintained the NK cell phenotypes (**Figure 18**). A low concentration (5 ng/ml) of IL-2 was sufficient for this suppression. Furthermore, the addition of IL-2 at 36 hours after culture initiation partially blocked the myeloid cell production (**Figure 19**), supporting that the inhibition by IL-2 is not due to NK-stimulating cytokine-mediated outgrowth of NK cells at the expense of myeloid progenitor differentiation. Moreover, M-medium-treated c-Kit$^+$CD24$^+$ NK cells included monocytes and neutrophils with ring-shaped or segmented nuclei, whereas activated lymphocytes containing large cytotoxic

granules were observed in M-medium supplemented with IL-2 (**Figure 20A**). In addition, the c-Kit^{+}CD24^{+} NK cells acquired functions as phagocytes and T cell-stimulating antigen-presenting cells by M-medium culture, but IL-2 inhibited the differentiation of the NK cells into functional myeloid cells (**Figure 20B, C**). Finally, I examined whether the converted c-Kit^{+}CD24^{+} NK cells maintained the NK cell function. IL-2 addition still maintained NK cell effector functions such as IFN-γ production and CD107a degranulation in response to cytokine or YAC-1 stimulation. M-medium-cultured c-Kit^{+}CD24^{+} NK cells expressed CD107a and produced IFN-γ from the beginning, but did not respond to NK cell stimuli (**Figure 20D**). These results suggest that although M-medium-treated c-Kit^{+}CD24^{+} NK cells could still express some effector molecules presumably due to the remaining mRNAs, they lost their NK cell-specific response ability upon stimulation during their lineage conversion into functional myeloid cells.

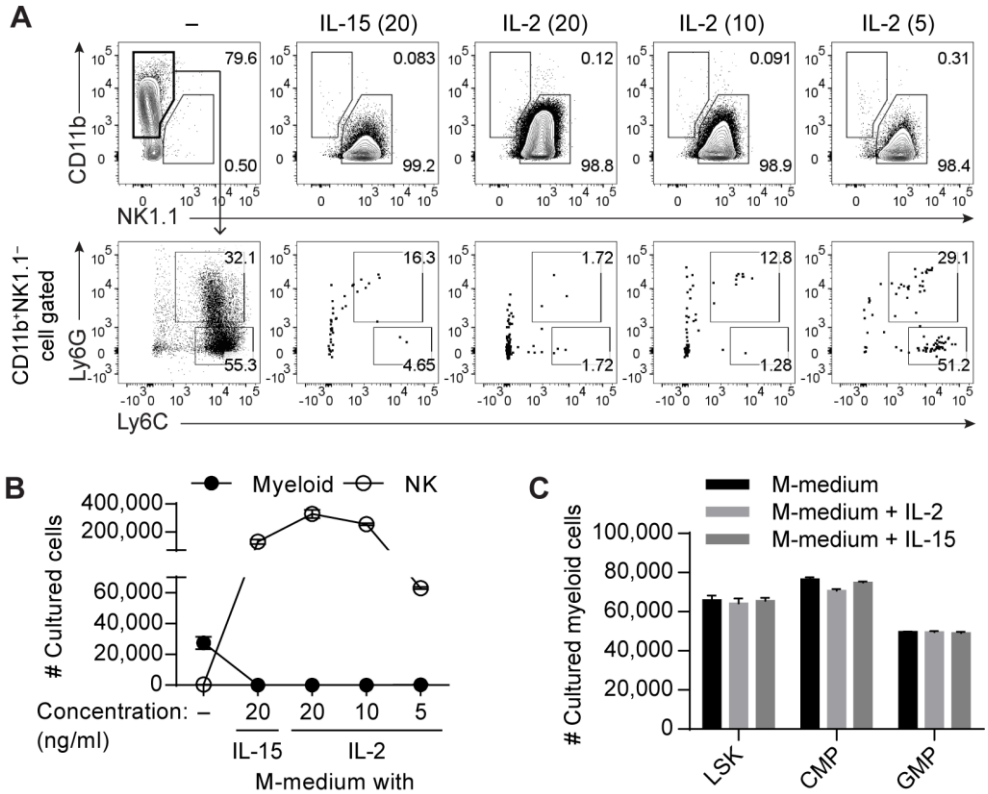

Figure 18. NK-stimulating cytokines inhibit the differentiation of c-Kit$^+$CD24$^+$ NK cells into myeloid cells in a dose-dependent manner

(**A**) Flow cytometric analysis of NK/myeloid cell phenotypes on C57BL/6 BM-derived c-Kit$^+$CD24$^+$ NK cells after 5 days in M-medium culture with IL-2 or IL-15. (**B**) The number of produced NK1.1$^+$CD122$^+$ NK cells and myeloid cells (neutrophil, monocytes, and macrophages) were quantified. (**C**) Quantification of myeloid cell production from HSPCs (LSK, CMP, and GMP) after 5 days in M-medium culture with 20 ng/ml of IL-2 or IL-15. Data represent at least two independent experiments.

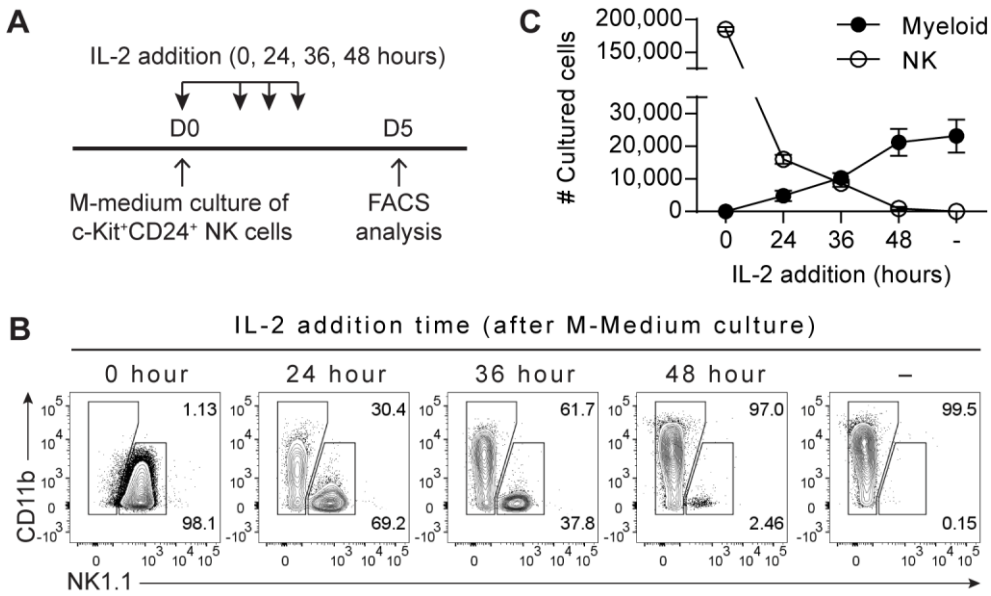

Figure 19. IL-2 blocks the conversion of c-Kit$^+$CD24$^+$ NK cells into myeloid cells

(**A**) Sorted c-Kit$^+$CD24$^+$ NK cells from naïve C57BL/6 BM were cultured in M-medium. IL-2 (20 ng/ml) was added at the indicated time points. After 5 days of cell culture, NK and myeloid cells were analyzed by flow cytometry (**B**) and quantified (**C**). Data represent three independent experiments.

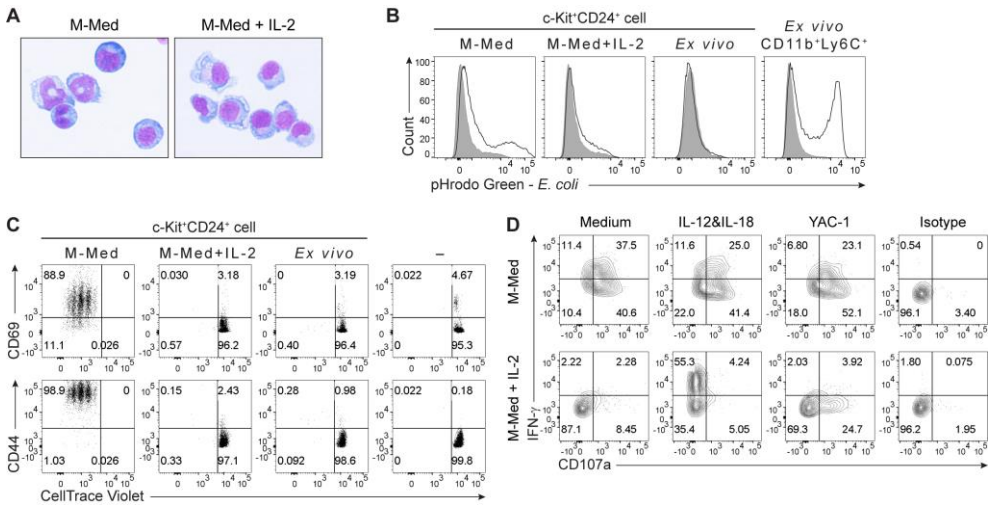

Figure 20. IL-2 inhibits the development of functional myeloid cells from c-Kit$^+$CD24$^+$ NK cells

(**A**) Photographs of Diff-Quik-stained C57BL/6 BM c-Kit$^+$CD24$^+$ NK cells cultured in M-medium with or without IL-2 for 5 days at a magnification of 200X. (**B**) Uptake of pHrodo Green *E. coli* bioparticles by C57BL/6 BM c-Kit$^+$CD24$^+$ NK cells differentiated with M-medium in the absence or presence of IL-2 for 8 days. *Ex vivo* CD11b$^+$Ly6C$^+$ cells were used as a positive control. These cells were incubated with the bioparticles at 37 ℃ (open) or 4 ℃ (filled) for 1.5 hours and phagocytosis was assessed through flow cytometry. (**C**) Proliferation and activation of OT-II-derived naïve CD4$^+$ T cells in the presence or absence of D8-cultured or *ex vivo* C57BL/6 BM c-Kit$^+$CD24$^+$ NK cells after co-incubation for 4 days. (**D**) IFN-γ production and CD107a degranulation in D7-cultured C57BL/6 BM c-Kit$^+$CD24$^+$ NK cells

stimulated with cytokines (IL-12 and IL-18) or YAC-1 cells for 4 hours. Data represent three (A−C) or two (D) independent experiments.

c-Kit$^+$CD24$^+$ NK cells are converted into neutrophils and monocytes *in vivo*

To investigate whether the myeloid cell production from c-Kit$^+$CD24$^+$ NK cells also occurs *in vivo*, I purified CD11b$^{low/+}$CD27$^+$ NK cells based on c-Kit and CD24 expression, and transferred them into CD45.1$^+$ TC-1 tumor-bearing mice. At 6 days after NK cell transfer, the majority of transferred c-Kit$^+$CD24$^+$ NK cells maintained the NK cell phenotype (**Figure 21A, B**). However, some of the c-Kit$^+$CD24$^+$ NK cells differentiated into tumor-associated neutrophils and monocytes in the BM (**Figure 21A, C**). Unlike *in vitro* experiments, c-Kit$^-$CD24$^-$ NK cells also produced myeloid cells, although the number of myeloid cells derived from c-Kit$^-$CD24$^-$ NK cells was less than that from c-Kit$^+$CD24$^+$ NK cells (**Figure 21C−E**). In addition, I found that c-Kit and CD24 were downregulated in transferred c-Kit$^+$CD24$^+$ NK cells retaining the NK phenotype, whereas c-Kit$^-$CD24$^-$ NK cells gained their expression, similar to that from endogenous NK cells (**Figure 21F**).

Next, to examine whether c-Kit$^+$CD24$^+$ NK cells also differentiate into myeloid cells in naïve mice, c-Kit$^+$CD24$^+$ or c-Kit$^-$CD24$^-$ NK cells were adoptively transferred into naïve CD45.1$^+$ mice. Similarly, some of the transferred c-Kit$^+$CD24$^+$ NK cells produced myeloid cells (**Figure 22A−E**). However, the myeloid cell production of c-Kit$^+$CD24$^+$ NK cells relative to c-

Kit^{-}CD24^{-} NK cells was reduced compared with that in tumor-bearing recipients (**Figure 21D** and **Figure 22D**), suggesting that the tumor environment promotes the differentiation of c-Kit^{+}CD24^{+} NK cells into myeloid cells. However, *in vivo* production of myeloid cells from transferred c-Kit^{-}CD24^{-} NK cells was still observed in naïve recipients (**Figure 22C−E**). Consistent with the results from tumor-bearing recipients, both unconverted c-Kit^{-}CD24^{-} and c-Kit^{+}CD24^{+} NK cells also similarly showed altered expression of c-Kit and CD24 in naïve recipients (**Figure 21F** and **Figure 22F**), supporting the variability of c-Kit and CD24 expression depending on the surrounding environment.

To examine which stimuli received by transferred NK cells adjusted the expression patterns of c-Kit and CD24 *in vivo*, sorted NK cells were cultured in the presence of several cytokines involved in NK survival/activation or the tumor immunosuppressive environment. The resultant c-Kit and CD24 expression patterns were variable and cytokine-dependent regardless of the initial expression (**Figure 23**). c-Kit is upregulated in the absence of cytokines, but IL-15 and IL-2 maintain c-Kit expression at *ex vivo* levels during NK cell stimulation for 44 hours [27]. However, I found that the IL-15/IL-2-induced downregulation of c-Kit was weakened after 5 days of cell culture (**Figure 23A**). Consistent with previous reports [28,29], IL-18 increased c-Kit expression.

IL-10 also upregulated c-Kit expression, whereas IL-4, IL-12, and TGF-β showed decreased expression (**Figure 23**). CD24 were downregulated after stimulation with IL-15, IL-2, and IL-18 but slightly upregulated by IL-10 (**Figure 23**). Collectively, these data might suggest that *in vivo* microenvironments can affect c-Kit and CD24 expression in NK cells and consequently change their potential for differentiation into myeloid cells [30].

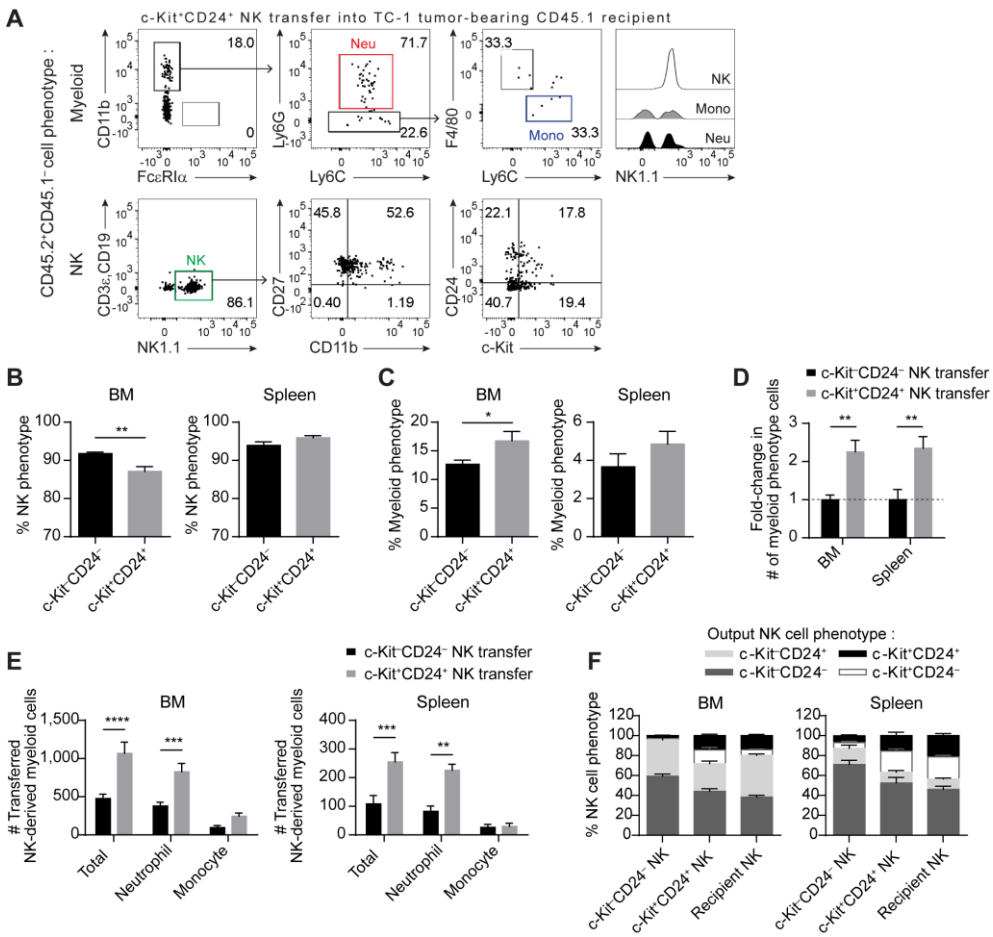

Figure 21. c-Kit$^+$CD24$^+$ NK cells generate myeloid cells *in vivo*

c-Kit$^+$CD24$^+$ or c-Kit$^-$CD24$^-$ NK cells derived from C57BL/6 mice were injected into TC-1 tumor-bearing CD45.1$^+$ C57BL/6 mice (2×10^5 NK cells per mouse; n=4 and 6, respectively). At 6 days after NK cell transfer, phenotype of transferred CD45.1$^-$CD45.2$^+$ NK cells was assessed in the BM and spleen. (**A**) Flow-cytometric analysis of myeloid and NK phenotypes of transferred NK cells from the BM. (**B, C**) Quantification of the phenotypes in

transferred NK cells from the BM and spleen. Myeloid phenotype cells include $CD11b^{+}Ly6G^{+}$ neutrophils, $CD11b^{+}Ly6G^{-}Ly6C^{+}IA/IE^{-}$ monocytes, $CD11b^{+}Ly6G^{-}Ly6C^{+}IA/IE^{+}$ moDCs, and $CD11b^{+}Ly6G^{-}Ly6C^{-}IA/IE^{+}F4/80^{+}$ macrophages. NK phenotype cells are $CD3/CD19^{-}NK1.1^{+}$ cells. (**D**) Quantification of the myeloid cell production from $c\text{-}Kit^{+}CD24^{+}$ NK cells. The fold-change values were calculated by setting the average number of myeloid phenotype cells derived from $c\text{-}Kit^{-}CD24^{-}$ NK cells to 1.0. (**E**) The number of transferred cells with the myeloid phenotype. (**F**) c-Kit and CD24 expression in unconverted NK cells. Recipient $CD11b^{+}CD27^{+}$ NK cells were used for endogenous control to show the tissue-specific expression. Data represent four independent experiments. * p-value<0.05, ** p-value<0.01, *** p-value<0.001, **** p-value<0.0001 by Mann-Whitney test (B, C) or two-way ANOVA (D, E).

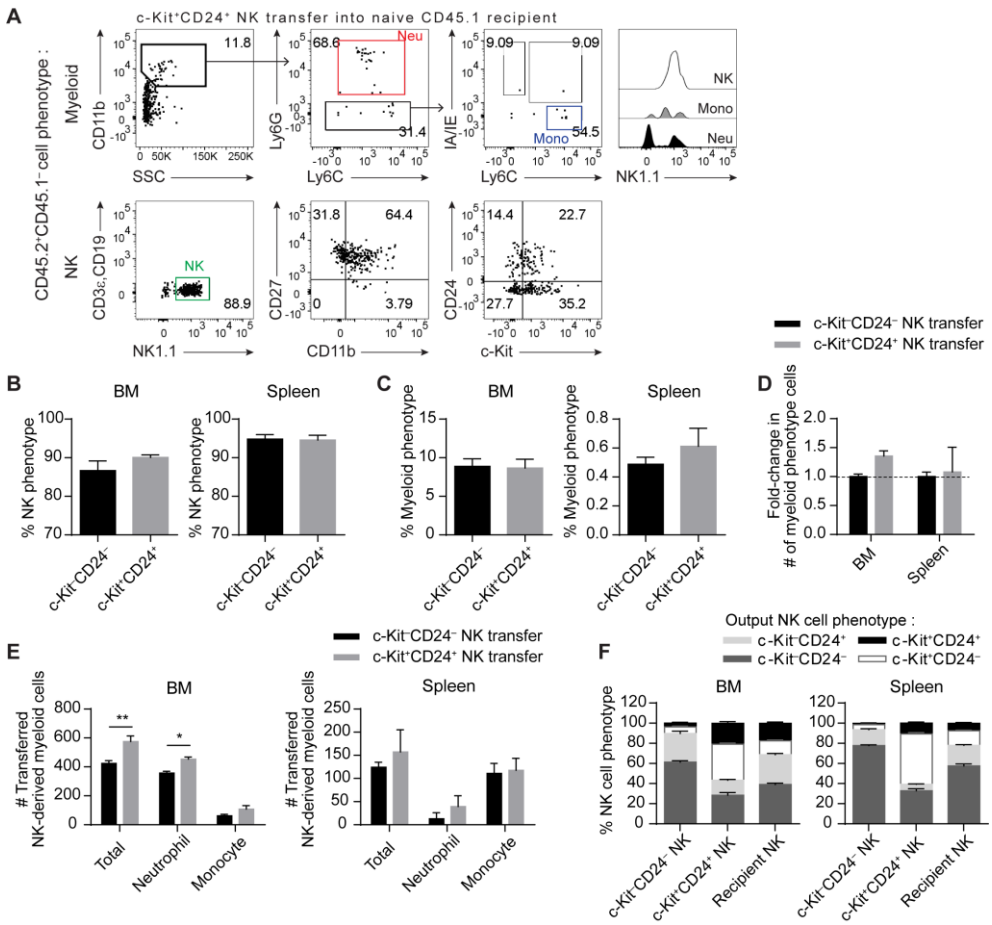

Figure 22. c-Kit$^+$CD24$^+$ NK cells also differentiate myeloid cells in a steady state

Naïve CD45.1$^+$ mice were intravenously injected with c-Kit$^+$CD24$^+$ or c-Kit$^-$CD24$^-$ NK cells derived from naïve C57BL/6 mice (3.5×10^5 NK cells per mouse; n=4 per group). After 6 days, NK cell differentiation was assessed in the BM and spleen. (**A**) Flow-cytometric analysis of myeloid and NK phenotypes of transferred NK cells from the BM. (**B**, **C**) Quantification of the

phenotypes in transferred NK cells from the BM and spleen. Cells with a myeloid phenotype cells include $CD11b^{+}Ly6G^{+}$ neutrophils, $CD11b^{+}Ly6G^{-}Ly6C^{+}IA/IE^{-}$ monocytes, $CD11b^{+}Ly6G^{-}Ly6C^{+}IA/IE^{+}$ moDCs, and $CD11b^{+}Ly6G^{-}Ly6C^{-}IA/IE^{+}F4/80^{+}$ macrophages derived from transferred NK cells. NK phenotype cells are $CD3/CD19^{-}NK1.1^{+}$ cells. (**D**) Quantification of the relative conversion of $c\text{-}Kit^{+}CD24^{+}$ NK cells into myeloid cells. The fold-change values were calculated by setting the average number of myeloid phenotype cells derived from $c\text{-}Kit^{-}CD24^{-}$ NK cells to 1.0. (**E**) The number of transferred cells with a myeloid phenotype. (**F**) Quantification of flexible c-Kit and CD24 expression in unconverted NK cells. Their expression in recipient $CD11b^{+}CD27^{+}$ NK cells was used to show the endogenous expression pattern. Data represent two independent experiments. * p-value<0.05, ** p-value<0.01 by two-way ANOVA (E).

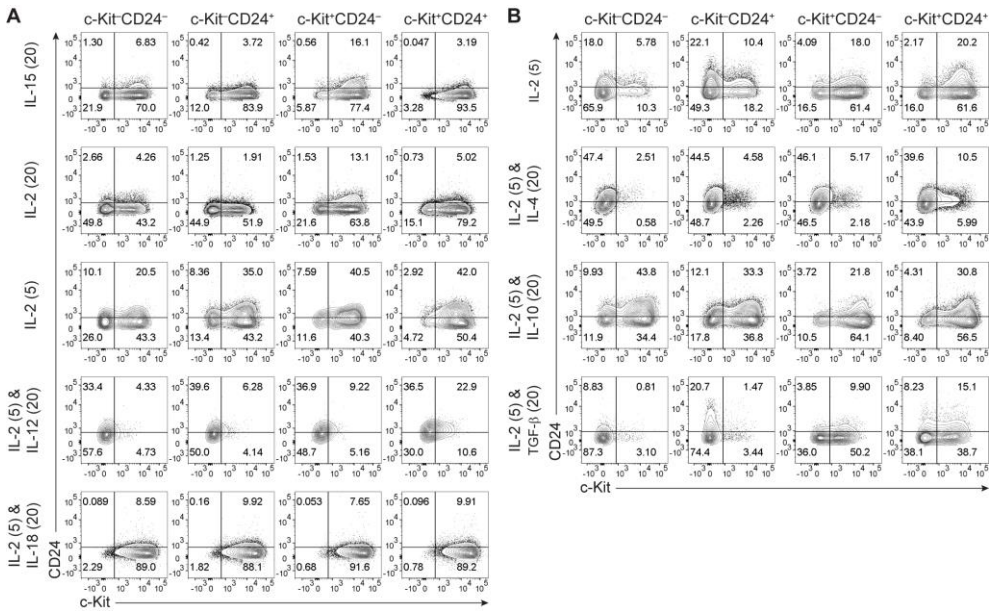

Figure 23. Cytokines direct NK cells toward cytokine-dependent phenotypes regardless of initial c-Kit and CD24 expression

NK cells from naïve C57BL/6 mice were separately sorted into four populations based on c-Kit and CD24 expression. The NK cells were cultured with the indicated cytokines for survival and activation of NK cells (**A**) or in the tumor immunosuppressive environment (**B**), and the phenotypic change in c-Kit and CD24 expression was evaluated after 5 days. Numbers in () indicate the concentrations of cytokines (ng/ml). Data represent three (A) or two (B) independent experiments.

c-Kit^{+}CD24^{+} NK cells maintain NK cell characteristics

To examine the cellular identity of myeloid-producible c-Kit^{+}CD24^{+} NK cells, I compared the gene expression profiles of c-Kit^{-}CD24^{-} and c-Kit^{+}CD24^{+} NK cells (**Figure 24A**). Both analyzed c-Kit^{-}CD24^{-} and c-Kit^{+}CD24^{+} NK cell samples hardly expressed other lineage-specific genes (**Figure 24B**). The transcriptome of c-Kit^{+}CD24^{+} NK cells was quite similar to that of c-Kit^{-}CD24^{-} NK cells, and there was no distinct difference in the profile of genes involved in NK cell function and development between c-Kit^{-}CD24^{-} and c-Kit^{+}CD24^{+} NK cells (**Figure 24C** and **Figure 25**). Flow-cytometric analysis revealed that c-Kit^{+}CD24^{+} NK cells followed the same expression patterns of transcription factors and cell-surface molecules as the other three NK cell populations (**Figure 26**).

To assess phenotypic heterogeneity among individual c-Kit^{+}CD24^{+} NK cells, tSNE analysis of c-Kit^{+}CD24^{+} NK cells was performed. c-Kit^{+}CD24^{+} NK cells homogeneously expressed NK cell markers (**Figure 27A**). Some of c-Kit^{+}CD24^{+} NK cells dimly expressed several myeloid cell markers, but their expression was also not correlated with NK cell marker expression (**Figure 27B**). Collectively, these results showed that in terms of expression of NK cell markers c-Kit^{+}CD24^{+} NK cells are a homogeneous NK cell population with heterogeneity of some myeloid cell markers.

Furthermore, in comparison to other NK cell populations, c-Kit^{+}CD24^{+} NK cells showed enhanced CD107a degranulation and IFN-γ production in response to IL-12/IL-18 or upon encountering NK-stimulating YAC-1 cells (**Figure 28**). Thus, c-Kit^{+}CD24^{+} NK cells maintained NK cell characteristics despite their differentiation potential into myeloid cells.

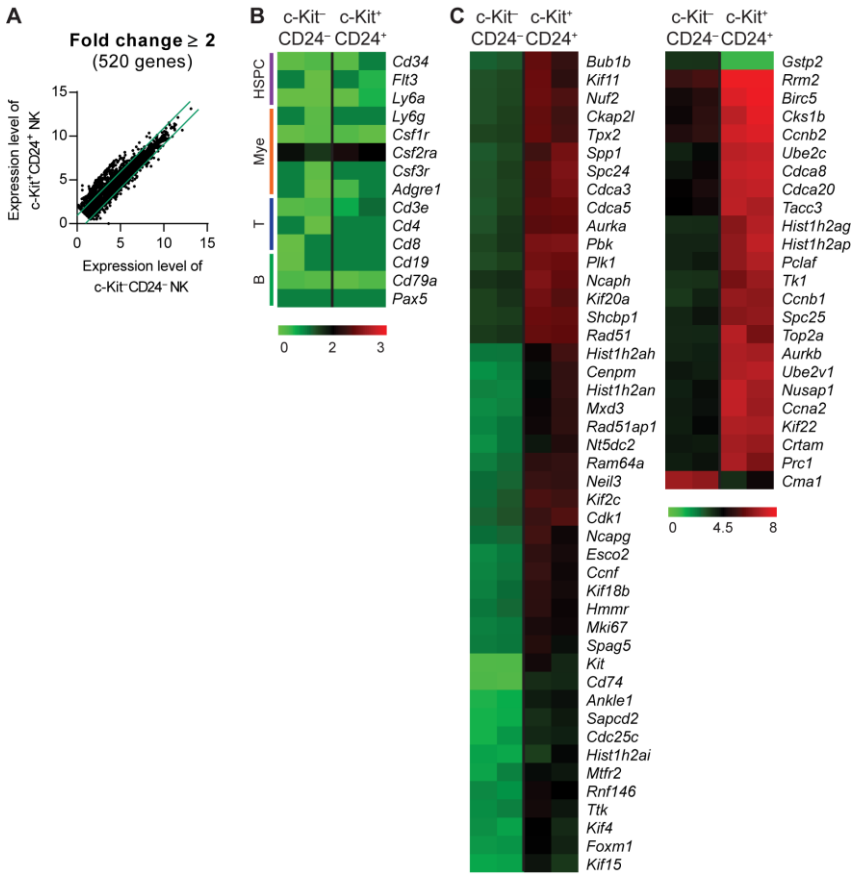

Figure 24. Comparative transcriptome analysis between c-Kit^{-}CD24^{-} and c-Kit^{+}CD24^{+} NK cells

(**A**) Differentially expressed gene analysis in c-Kit^{-}CD24^{-} NK cells versus c-Kit^{+}CD24^{+} NK cells. (**B**) Transcriptome profiles for hematopoietic cell lineage-related genes. (**C**) Heatmap showing differential expression of genes (change of ≥ 5.0-fold in c-Kit^{+}CD24^{+} NK/c-Kit^{-}CD24^{-} NK; upregulated genes (left) and downregulated genes (right)). (**B**, **C**) The color scale represents the log2 (FPKM+1).

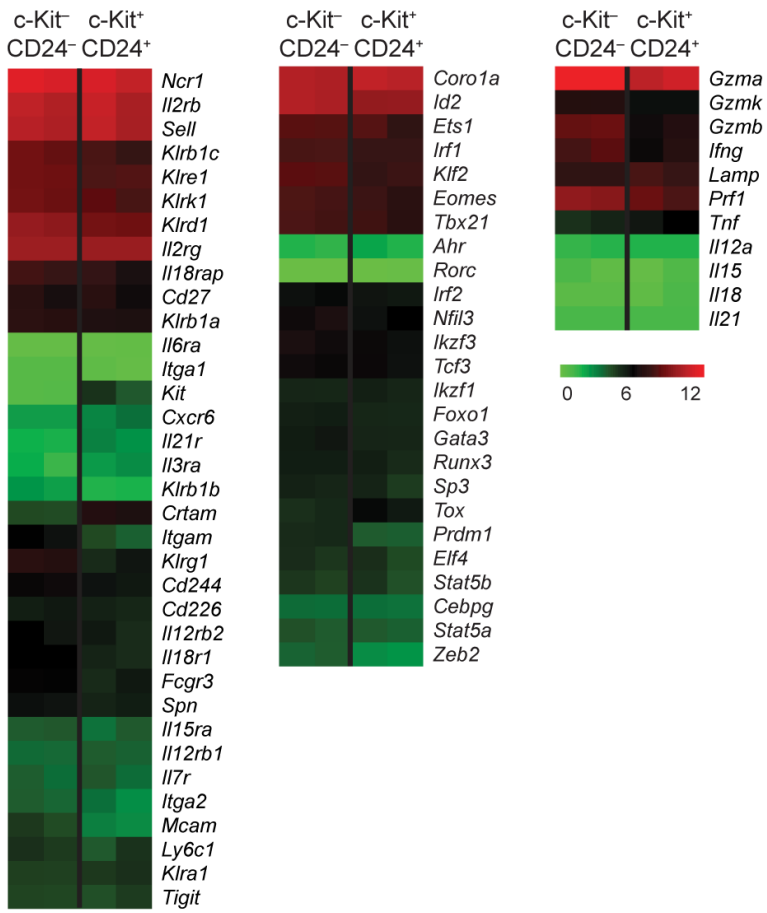

Figure 25. Transcriptome analysis reveals no difference in NK cell-related molecules between c-Kit^{-}CD24^{-} and c-Kit^{+}CD24^{+} NK cells

Heatmap of genes encoding NK-related surface molecules (left), transcription factors (middle), and effector molecules (right) in c-Kit^{-}CD24^{-} and c-Kit^{+}CD24^{+} NK cells. The color scale represents the log2 (FPKM+1).

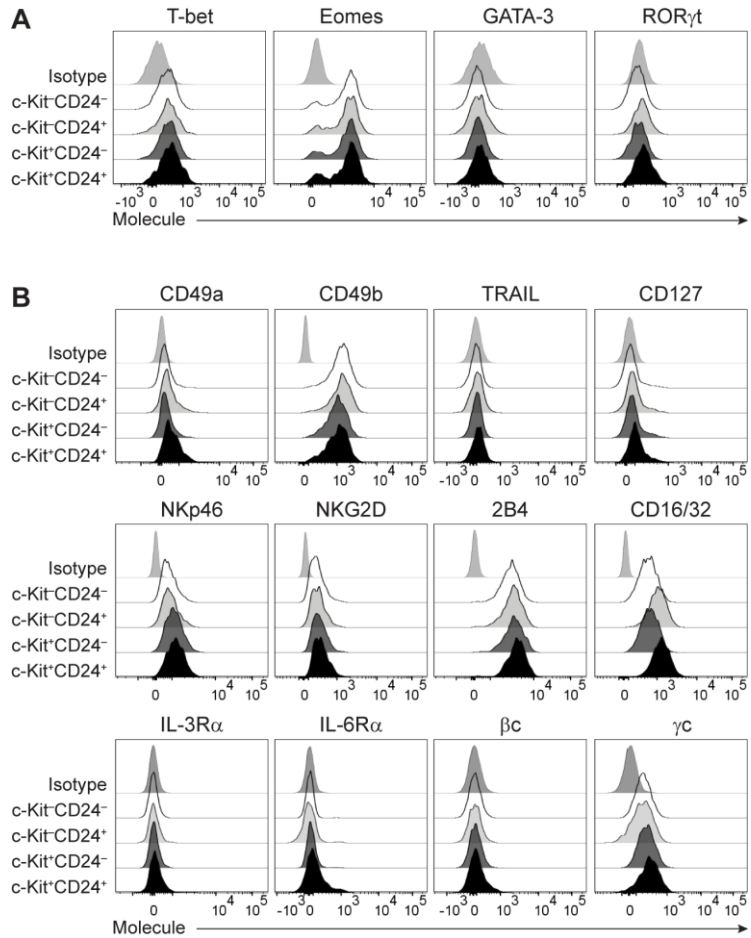

Figure 26. c-Kit$^+$CD24$^+$ NK cells maintain NK cell-specific phenotypic characteristics

Flow-cytometric analysis of expression of NK-related transcription factors (**A**) and surface markers (**B**) in BM NK cells from naïve C57BL/6 mice. Data represent three (A) or two (B) independent experiments.

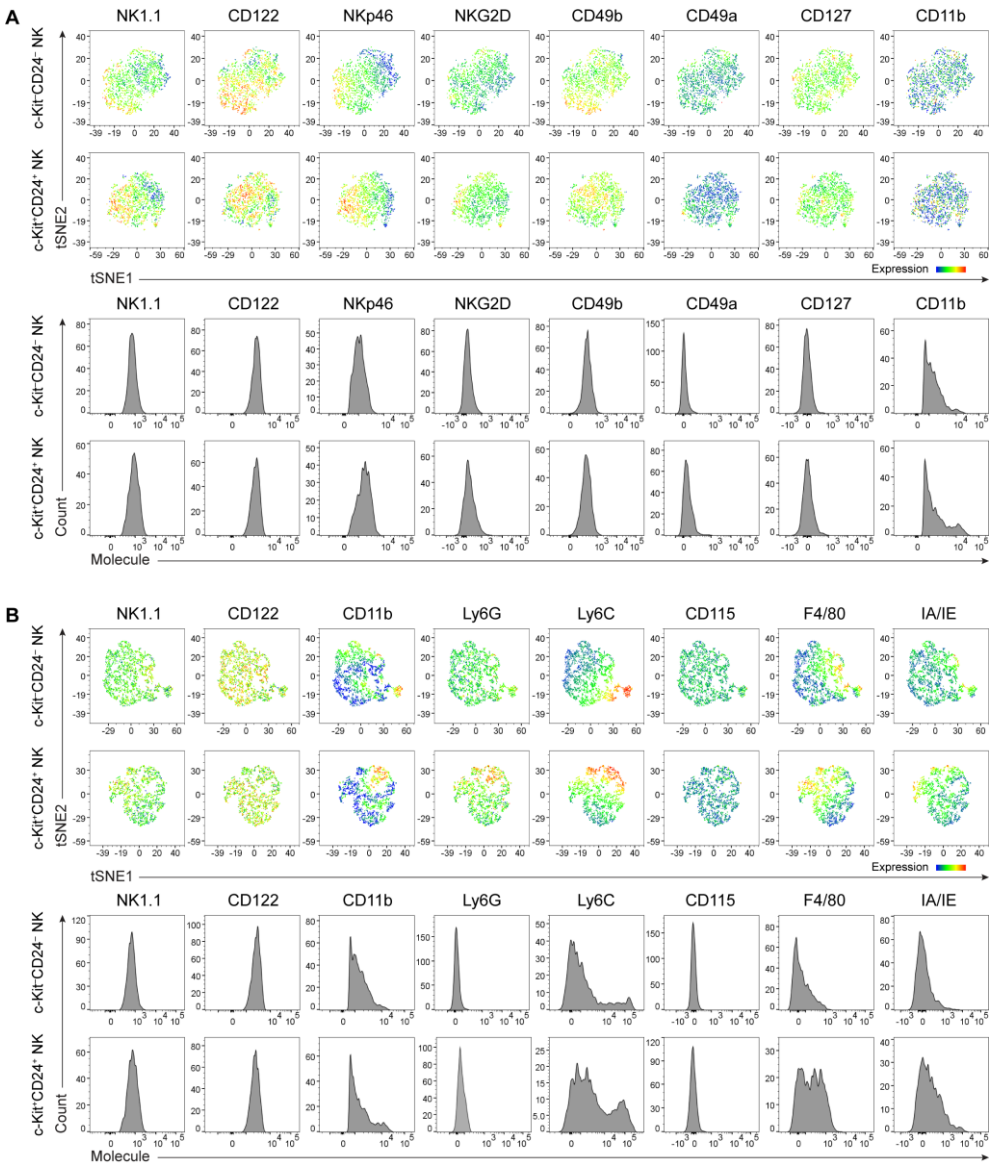

Figure 27. Homogeneity and heterogeneity of c-Kit$^+$CD24$^+$ NK cells

tSNE analysis and histogram plot of flow cytometry data from c-Kit$^-$CD24$^-$ or c-Kit$^+$CD24$^+$ NK cells derived from naïve C57BL/6 BM. The heatmap showing median expression of selected NK (**A**) and myeloid (**B**) markers on

the tSNE plot. Flow-cytometric analysis was done after excluding doublets. The overall phenotypes of analyzed NK cells are Lin(CD3ε/CD19/CD34/Ly6G)$^{-}$CD122^{+}NK1.1^{+}CD11b^{+}CD27^{+}c-Kit^{-}CD24^{-}, and Lin(CD3ε/CD19/CD34/Ly6G)$^{-}$CD122^{+}NK1.1^{+}CD11b^{+}CD27^{+}c-Kit^{+}CD24^{+}, respectively. Data represent two independent experiments.

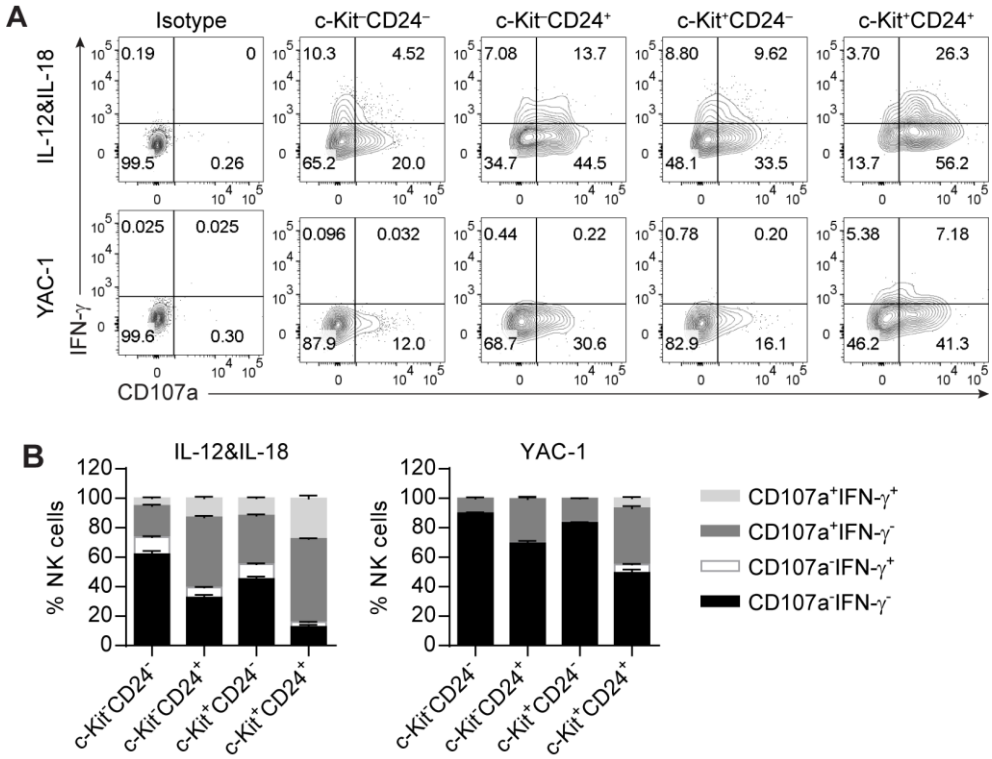

Figure 28. c-Kit$^+$CD24$^+$ NK cells maintain NK cell-specific functional characteristics

Flow-cytometric analysis (**A**) and quantification (**B**) of IFN-γ production and CD107a degranulation in naïve C57BL/6-derived BM NK cells stimulated with cytokines (IL-12 and IL-18) or YAC-1 cells for 4 hours. Data represent two independent experiments.

Distinctive interplay between transcription factors controls the myeloid cell development from c-Kit$^+$CD24$^+$ NK cells

Finally, to delineate the underlying mechanisms of myeloid cell production from c-Kit$^+$CD24$^+$ NK cells, changes in transcriptome profiles by M-medium culture were analyzed in c-Kit$^+$CD24$^+$ NK cells. Numerous transcription factor-encoding genes were significantly up- or downregulated during the M-medium culture (**Figure 29**; 331 genes with ≥ 4.0-fold change in M-Med 24 h/*Ex vivo* in c-Kit$^+$CD24$^+$ NK cells). Among the DEGs, genes encoding NK-related transcription factors, including T-bet (*Tbx21*), ETS1 (*Ets1*), and AP-1 subunits (*Fos*, *Jun*, and *Junb* etc.), were downregulated during the differentiation into myeloid cells (**Figure 29B**). I further examined protein-protein interaction networks to narrow the scope of candidates playing key roles in NK cell differentiation into myeloid cells (**Figure 30**). During M-medium culture, signaling through IFN-γ, TNF, and AP-1, involved in regulating the function and activation of NK cells, was greatly reduced. I confirmed expression of genes for NK and myeloid cells during the differentiation of c-Kit$^+$CD24$^+$ NK cells into myeloid cells. Expression of NK-related *Id2* and *Ets1* mRNA was substantially decreased in M-medium culture (**Figure 31A**), while expression of genes responsible for myeloid cell development (*Cebpa*, *Cebpb*, and *Spi1* (PU.1)) was increased (**Figure 31B**).

Additionally, IL-2 inhibited the M-medium-induced changes in the expression of NK/myeloid cell-related genes. These findings suggested that c-Kit$^+$CD24$^+$ NK cells temporarily go through an intermediate development stage where they exhibit both NK and myeloid lineage signatures before eventually turning into myeloid cells by M-medium treatment. However, addition of IL-2, an NK lineage-stimulating cytokine, can abrogate these changes in lineage programming.

Next, based on known functions in development and lineage commitment of hematopoietic cells, several transcription factors with high positive fold-change values and active interactions with other factors were selected, and their expression was confirmed by quantitative PCR. *Gata2*, *Gfi1b*, *Lmo2*, *Meis1*, *Nfe2*, and *Spi1* mRNA were upregulated and then declined during the differentiation of c-Kit$^+$CD24$^+$ NK cells into myeloid cells (**Figure 31C**). Expectedly, IL-2 also inhibited the upregulation of these candidate genes upon M-medium treatment. I also compared the gene expression kinetics of NK cells with those of HSPCs. Unlike c-Kit$^+$CD24$^+$ NK cells, these transcription factors were expressed in HSPCs before cell culture but were downregulated during myeloid cell development (**Figure 31D**), suggesting that the distinctive interplay between these factors controls the differentiation of c-Kit$^+$CD24$^+$ NK cells into myeloid cells.

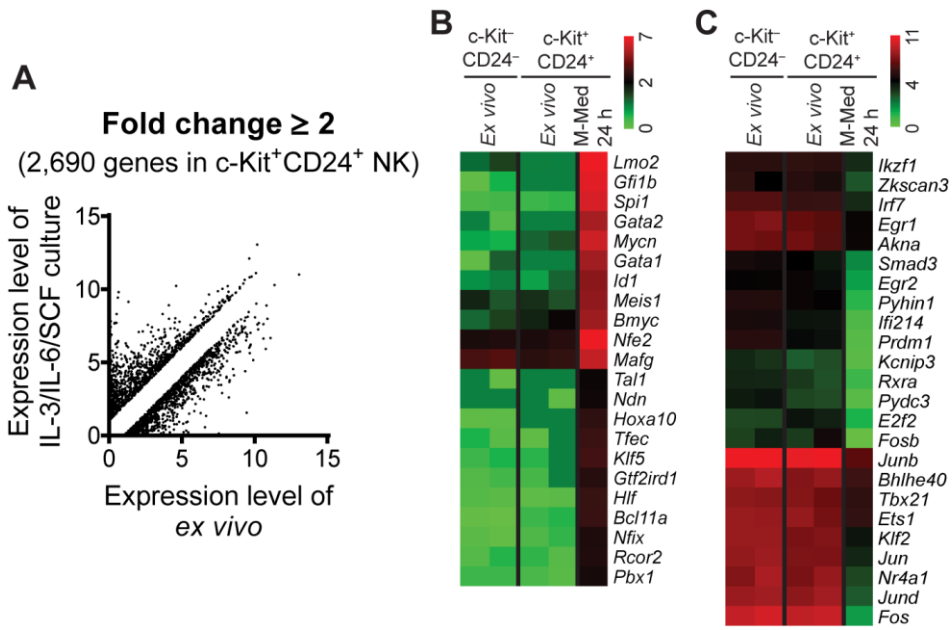

Figure 29. The change in expression of transcription factor-encoding genes in c-Kit$^+$CD24$^+$ NK cells during the conversion into myeloid cells

(**A**) RNA sequencing analysis of gene expression during conversion of c-Kit$^+$CD24$^+$ NK cells induced by M-medium treatment for 24 hours. (**B**, **C**) Transcriptome analysis during the differentiation of c-Kit$^+$CD24$^+$ NK cells induced by M-medium treatment for 24 hours. Heatmap of upregulated (**B**) and downregulated (**C**) genes encoding transcription factors (≥ 4.0-fold change in c-Kit$^+$CD24$^+$ NK cells during M-medium culture) is shown. The color scale represents the log2 (FPKM+1).

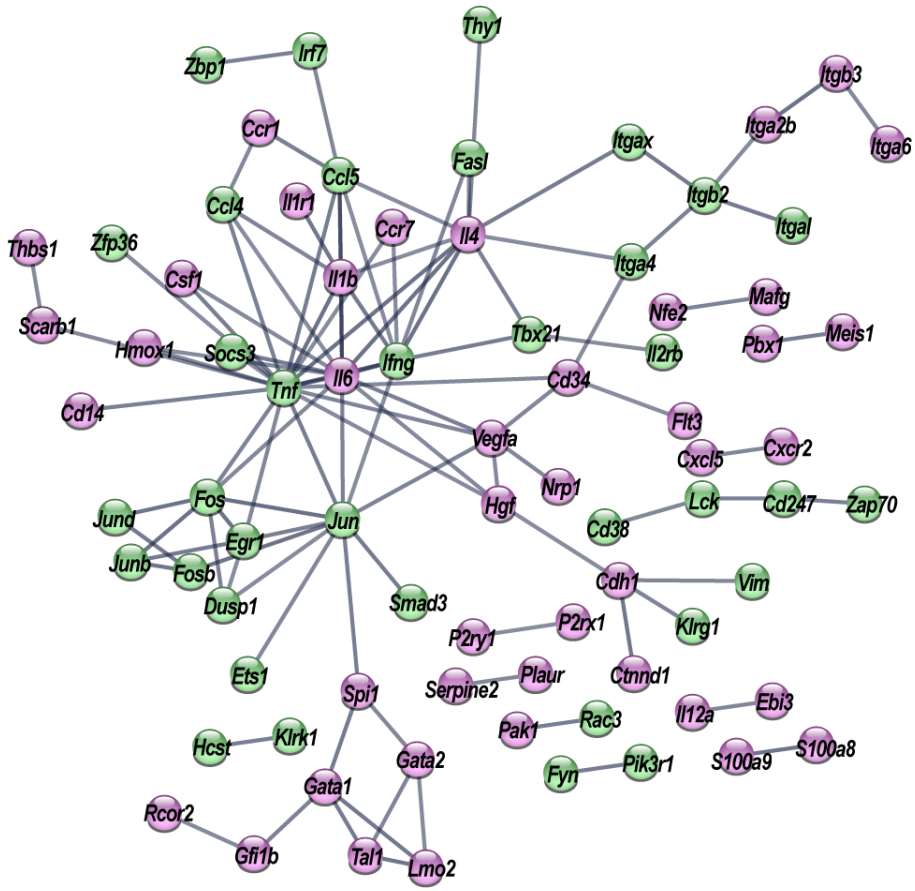

Figure 30. Protein-protein interaction network during conversion of c-Kit^{+}CD24^{+} NK cells into myeloid cells

Protein-protein interactions among DEGs encoding transcription factors and signaling molecules with fold-change ≥ 4.0 (M-Med 24h/*Ex vivo* in c-Kit^{+}CD24^{+} NK cells) were analyzed through the STRING database (high confidence). Pink and green indicates upregulated and downregulated genes, respectively.

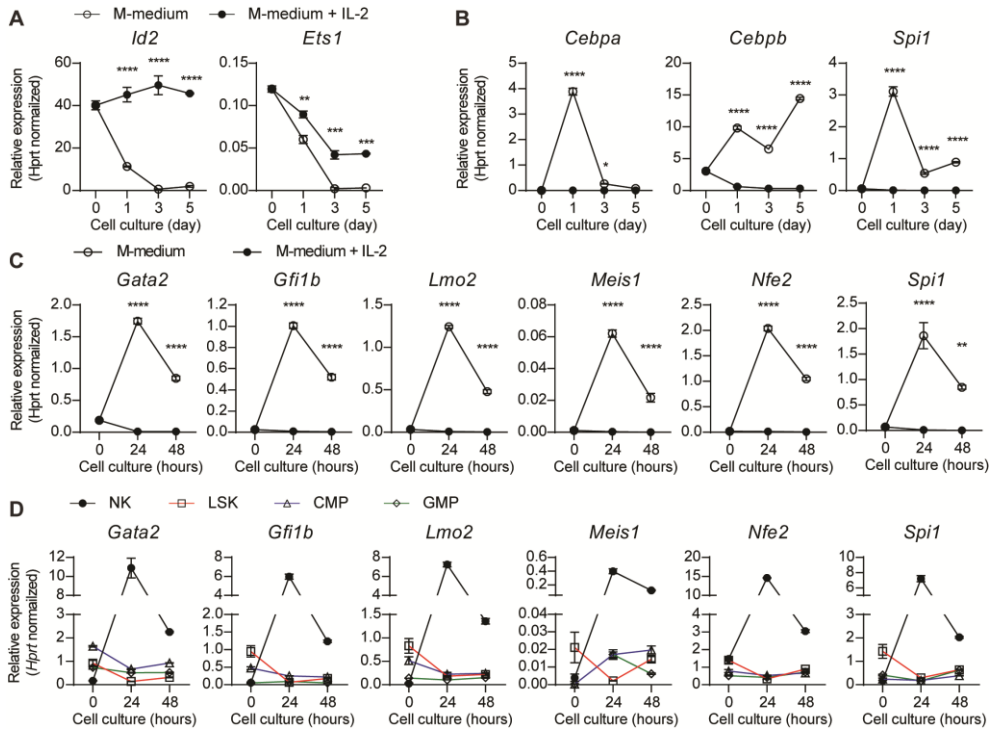

Figure 31. Numerous transcription factors are regulated during the differentiation of c-Kit$^+$CD24$^+$ NK cells into myeloid cells

(**A**, **B**) Quantification of the expression of genes encoding transcription factors involved in NK cell (**A**) or myeloid cell (**B**) development during M-medium culture of C57BL/6 BM-derived c-Kit$^+$CD24$^+$ NK cells in the absence or presence of IL-2. (**C**) Quantification of the expression of genes encoding transcription factors involved in lineage commitment and/or reprogramming during M-medium-induced differentiation of BALB/c BM-derived c-Kit$^+$CD24$^+$ NK cells in the absence or presence of IL-2. (**D**) Quantification of the expression of the genes from C57BL/6 BM-derived c-

$Kit^{+}CD24^{+}$ NK cells and HSPCs (LSK, CMP, and GMP) during M-medium culture. Data represent two (A, B) or three independent experiments (C, D). * p-value<0.05, ** p-value<0.01, *** p-value<0.001, **** p-value<0.0001 by two-way ANOVA (A−D).

GATA-2 is necessary for differentiation of c-Kit$^+$CD24$^+$ NK cells into myeloid cells

Because GATA-2 is an upstream regulator of Gfi-1b and PU.1, cooperating with LMO-2 during lineage specification of hematopoietic cells [31-33], I further examined the role of GATA-2 in the differentiation of c-Kit$^+$CD24$^+$ NK cells into myeloid cells by using chemical inhibitors that repress GATA-2 activity. Treatment of K-7174, a GATA-specific inhibitor, hampered the myeloid cell production of c-Kit$^+$CD24$^+$ NK cells by abrogating *Gata2* upregulation, but it also caused severe cytotoxicity at a high concentration (**Figure 32** and **Figure 33A, C**). To definitively confirm the GATA-2-dependent differentiation of c-Kit$^+$CD24$^+$ NK cells into myeloid cells, I treated the NK cells with mitoxantrone, a novel unharmful GATA-2-specific inhibitor [34] (**Figure 32**). As a result, mitoxantrone also suppressed the myeloid cell production from c-Kit$^+$CD24$^+$ NK cells through inhibition of *Gata2* upregulation by M-medium treatment (**Figure 33B, D**).

Finally, to demonstrate the role of GATA-2 in the myeloid cell development from NK cells, I performed GATA-2-overexpressing experiments. GATA-2 transduction still did not affect survival and subsequent differentiation of myeloid-u producible c-Kit$^-$ NK cells under M-medium culture (**Figure 34A**). However, the number of GFP$^+$ myeloid cells

doubled by transduction of GATA-2 into myeloid-producible c-Kit^{+} NK cells compared with that of the control (**Figure 34B−D**). In conclusion, GATA-2 is necessary but not sufficient for the differentiation of c-Kit^{+}CD24^{+} NK cells into myeloid cells.

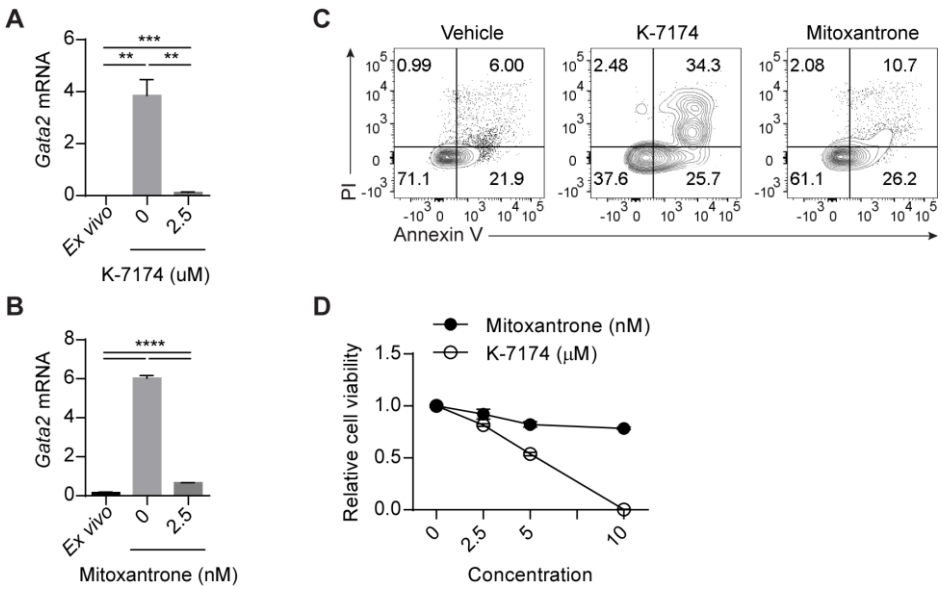

Figure 32. GATA-2 inhibitors differentially affect apoptosis of NK cells

(**A**, **B**) C57BL/6 BM-derived c-Kit^{+}CD24^{+} NK cells were cultured in M-medium in the presence or absence of K-7174 (**A**) or mitoxantrone (**B**). After 36 hours, *Gata2* mRNA expression was quantified. (**C, D**) C57BL/6 BM NK cells were cultured with IL-2 (10 ng/ml) in the presence or absence of GATA-2 inhibitors. After 4 days, cell apoptosis was determined by Annexin V and PI staining. (**C**) Representative results for NK cell apoptosis following treatment with 5 μM K-7174 or 5 nM mitoxantrone. (**D**) The relative cell viability values were calculated by setting the % Annexin V^{-}PI^{-} live cells from the no-treatment control to 1.0. Data represent two independent experiments. ** p-value<0.01, *** p-value<0.001, **** p-value<0.0001 by the Student's t test.

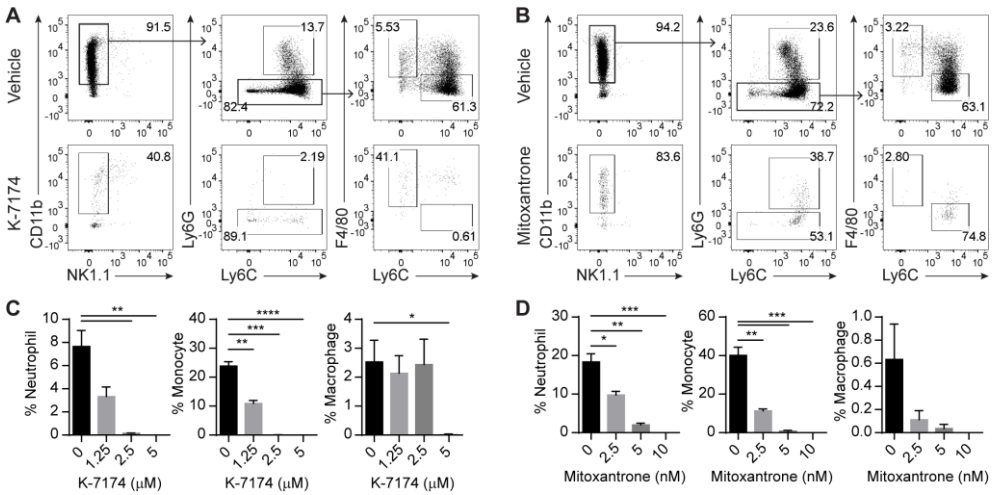

Figure 33. GATA-2 inhibitors suppress the conversion of c-Kit$^+$CD24$^+$ NK cells into myeloid cells in a dose-dependent manner

(**A**, **B**) C57BL/6 BM-derived c-Kit$^+$CD24$^+$ NK cells were cultured in M-medium in the presence of 2.5 μM GATA inhibitor K-7174 (**A**) or 2.5 nM GATA-2 inhibitor mitoxantrone (**B**). After 5 days, myeloid cell production from the NK cells was assessed by flow cytometry. (**C**, **D**) C57BL/6 BM-derived c-Kit$^+$CD24$^+$ NK cells were cultured in M-medium in the presence of K-7174 (**C**) or mitoxantrone (**D**) at various concentrations for 5 days, and the frequency of myeloid cells generated from c-Kit$^+$CD24$^+$ NK cells was analyzed. Data represent three independent experiments. * p-value<0.05, ** p-value<0.01, *** p-value<0.001, **** p-value<0.0001 by the Student's t test (B, D).

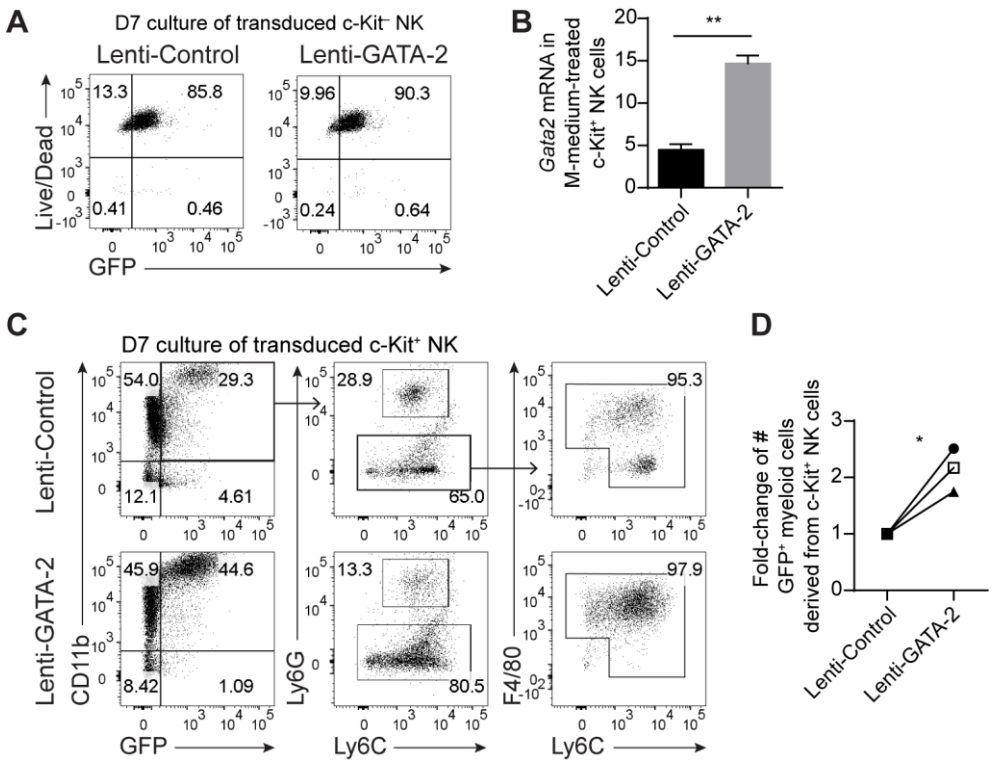

Figure 34. GATA-2 overexpression increases the differentiation of c-Kit$^+$ NK cells into myeloid cells

GATA-2 overexpression in C57BL/6 BM-derived c-Kit$^-$ or c-Kit$^+$ NK cells through lentiviral transduction (GFP as the transduction marker). (**A**) GATA-2 or control lentivirus-transduced c-Kit$^-$ NK cells were cultured in M-medium, and cell viability was assessed after 7 days. (**B**–**D**) GATA-2 or control lentivirus-transduced c-Kit$^+$ NK cells were cultured in M-medium. (**B**) Expression of *Gata2* mRNA in lentivirus-transduced c-Kit$^+$ NK cells which were cultured in M-medium for 36 hours. (**C**) Flow cytometric analysis of the

myeloid phenotype from GFP^+ transduced NK cells after 7 days of M-medium culture. (**D**) The relative quantification of myeloid cells derived from GATA-2-transduced c-Kit^+ NK cells. The fold-change values were calculated by setting the number of GFP^+ myeloid cells derived from control-transduced c-Kit^+ NK cells to 1.0. Each symbol represents an individual experiment. Data represent three independent experiments. * p-value<0.05, ** p-value<0.01 by the Student's t test (B) or the paired t test (D).

Discussion

Although the manipulation of lineage specifiers induces lineage reprogramming between immune cells, naturally occurring lineage conversion is still poorly understood. Myeloid-committed progenitors are regarded as main sources of myeloid cell development. However, my data suggest that GATA-2-dependent differentiation of c-Kit^{+}CD24^{+} NK cells could contribute to myeloid cell development in physiological conditions.

Multipotent hematopoietic stem and progenitors were thought to commit to specific lineages and become progressively restricted in their lineage choices. In contrast, recent studies have identified that reversible lineage commitment can occur in fully differentiated cells in both healthy and pathogenic conditions. CD8^{+} T cells are reprogrammed into MHC class I-restricted CD4^{+}Foxp3^{+} regulatory T cells in the steady-state gut-associated microenvironment [35]. In tumor conditions, monocytic MDSCs are converted into polymorphonuclear MDSCs by epigenetic silencing of *Rb1* [36]. NK cells are converted into type 1 ILCs in the tumor environment and *Toxoplasma gondii* infection [37-39]. These natural examples indicate that the differentiation of NK cells into myeloid cells is not an improbable phenomenon. However, differentiated cells are commonly converted into adjacent lineages during the

naturally occurring lineage reprogramming between immune cells. Therefore, it is noteworthy that c-Kit^{+}CD24^{+} NK cells differentiates into distant myeloid lineages.

In this study, I found that among mature CD11b^{+}CD27^{+} NK cells, c-Kit^{+}CD24^{+} cells were capable of differentiating into myeloid cells. c-Kit and its ligand SCF are important for the survival, proliferation, maturation, and function of NK cells [40-42]. However, their functions were mainly studied in NK cells stimulated with cytokines such as IL-2, IL-15, or IL-12. In the absence of stimuli for NK cell survival, similar to my system, SCF signaling weakly enhances the capacity of CD56^{bright} NK cells to degranulate [27]. I observed that SCF alone could not induce differentiation of NK cells into myeloid cells, and at least the addition of IL-3 was required for the differentiation, indicating that SCF signaling via c-kit could lead to differentiation of NK cells into myeloid cells with the support of other stimuli.

With c-Kit, I also identified CD24 as an additional marker for NK cell populations that can differentiate into myeloid cells. The function of CD24 is less clear in many cell types due to its variable glycosylation and context-dependent ligand specificity [43,44]. However, recent studies have shown an indispensable role of CD24 in determining the pluripotent properties of stem

and progenitor cells [25,26], supporting that myeloid-producible NK cells are distinguished by the expression of CD24.

I confirmed the NK-origin of myeloid cells generated from M-medium culture of c-Kit^{+}CD24^{+} NK cells through NK lineage-tracing *Ncr1*$^{iCRE/WT}$*R26R*$^{EYFP/WT}$ mice. Further experiments revealed that highly pure (double-sorted) or activated c-Kit^{+}CD24^{+} NK cells also generated myeloid cells. The NK-stimulatory cytokines IL-2 and IL-15 inhibited the differentiation of c-Kit^{+}CD24^{+} NK cells into functional myeloid cells and induced the retention of phenotypes, morphologies, and function of NK cells. These findings completely excluded the possibility that myeloid cell production via c-Kit^{+}CD24^{+} NK cells was caused by contamination of myeloid progenitors. I also found that the c-Kit^{+}CD24^{+} NK cells differentiated into myeloid cells *in vivo* in the context of tumor environment and even at steady state. However, unlike the results from the *in vitro* experiments, conversion of c-Kit^{-}CD24^{-} NK cells into myeloid cells was also observed *in vivo*. While the *in vitro* culture system only provides limited cytokine stimulation, environmental factors such as interactions with neighboring cells might have contributed to the conversion of some of the c-Kit^{-}CD24^{-} NK cells into myeloid cells *in vivo*.

Although the bulk of c-Kit^{+}CD24^{+} NK cells showed NK cell characteristics, such as NK-specific phenotypes and the production of effector molecules, and individual c-Kit^{+}CD24^{+} NK cells analyzed through tSNE also quite homogenously expressed NK cell markers, controversy persists concerning the cellular and developmental identity of myeloid-producible NK cells. Some of early lymphoid progenitors still retain myeloid lineage potential [45-48]. c-Kit^{+}CD24^{+} NK cells also might intrinsically possess NK- and myeloid-lineage potential as a common NK/myeloid progenitor population. In NK cell development, however, expression of CD122 marks the full commitment of CLPs into NK cell progenitors and subsequent acquisition of NKG2D, NK1.1, NKp46, and CD49b indicates the irreversible fate decision into the NK cell lineage [49]. Functional maturation of NK cells is defined by sequential changes in the surface expression of CD11b and CD27 (CD11b^{-}CD27^{-} → CD11b^{-}CD27^{+} → CD11b^{+}CD27^{+} → CD11b^{+}CD27^{-}) [50]. Based on the information, the phenotype of myeloid-producible NK cells (Lin^{-}CD122^{+}NK1.1(or NKp46)$^{+}$CD11b^{+}CD27^{+}c-Kit^{+}CD24^{+}) represents mature NK cells immediately before terminal differentiation. NK cells comprise a more heterogeneous population of cytotoxic ILCs than previously proposed, according to recent studies [51-55]. NK cells with a distinct myeloid signature have even been identified in adipose tissues [56]. When heterogeneity

of c-Kit^{+}CD24^{+} NK cells were assessed through tSNE analysis of flow cytometry data, c-Kit^{+}CD24^{+} NK cells were a quite homogeneous cell population in expression of NK cell markers. Although some of c-Kit^{+}CD24^{+} NK cells dimly expressed several myeloid cell markers, it has previously been reported that NK cells express several myeloid cell markers [56-61], suggesting that c-Kit^{+}CD24^{+} NK cells are a homogeneous NK cell population with heterogeneity of several myeloid cell markers. To further investigate these issues of identity and heterogeneity of c-Kit^{+}CD24^{+} NK cells, high dimensional single-cell analysis such as single cell RNA sequencing or mass cytometry will be required. Moreover, it still remains to be elucidated whether c-Kit^{+}CD24^{+} NK cells are a bipotent progenitor population, which can give rise to both NK and myeloid cells, or a heterogeneous population containing at least two subpopulations with NK- or myeloid-biased fates.

Interestingly, my transcriptome analysis demonstrated that the levels of *Gata2*, *Gfi1b*, *Lmo2*, *Meis1*, *Nfe2* and *Spi1*, involved in hematopoietic lineage specification and myeloid cell development, were significantly altered during the differentiation of c-Kit^{+}CD24^{+} NK cells into myeloid cells. Those genes were markedly upregulated after 24 hours of M-medium treatment, but promptly reduced. The expression kinetics were clearly distinguished from those of conventional HSPCs during normal myeloid cell development.

Notably, GATA-2 inhibitors blocked the differentiation of c-Kit$^+$CD24$^+$ NK cells into myeloid cells in a dose-dependent manner, and GATA-2 overexpression increased myeloid cell production from transduced c-Kit$^+$ NK cells. GATA-2 is mainly expressed in hematopoietic stem and progenitor cells and interacts with Gfi-1b, LMO-2, PU.1, and NF-E2 during the lineage commitment of hematopoietic cells [31-33]. Moreover, GATA-2 is also a well-characterized factor in lineage reprogramming [62-65]. For example, GATA-2 is necessary for the hemogenic endothelium to undergo endothelial-to-hematopoietic transition during embryonic hematopoiesis [62]. I demonstrated that GATA-2 is a necessary factor contributing to the differentiation of c-Kit$^+$CD24$^+$ NK cells into myeloid cells. Generally, however, several key factors are involved in both natural and induced lineage conversion [62-66], suggesting that other factors can play an important role in the differentiation of NK cells into myeloid cells by cooperating with GATA-2 directly or indirectly. Furthermore, the underlying molecular mechanism of the GATA-2-dependent differentiation remains to be clarified.

During the conversion of the c-Kit$^+$CD24$^+$ NK cells into myeloid cells by M-medium treatment, expression of the NK phenotype marker and genes encoding NK-related transcription factors were gradually downregulated. Meanwhile, the expression of the myeloid cell markers and genes involved in

the myeloid cell development dramatically increased early during the differentiation and then were maintained thereafter. Morphologically, M-medium-treated c-Kit$^+$CD24$^+$ NK cells had band-shaped or segmented nuclei, which is a characteristic feature of myeloid cells. Functionally, c-Kit$^+$CD24$^+$ NK cells with the NK-specific effector functions were converted into functional myeloid cells with phagocytosis and antigen presentation abilities, but they lost the NK-like responsiveness to NK stimuli. The addition of NK-stimulatory cytokines completely inhibited the changes in the phenotype, gene expression, morphology, and function of c-Kit$^+$CD24$^+$ NK cells that were mediated by the M-medium treatment. Collectively, the results indicate that the c-Kit$^+$CD24$^+$ NK cells temporarily go through an intermediate development stage where they exhibit both NK and myeloid lineage signatures as well as express the transcription factors involved in lineage commitment and reprogramming. Subsequently, these cells lose their NK cell identity and get converted into functional myeloid cells by M-medium treatment.

While the M-medium-treated c-Kit$^+$CD24$^+$ NK cells lost phenotype, ability to express genes encoding NK-related transcription factors, morphology, and function of typical NK cells, they acquired the phenotypic, transcriptional, morphological, and functional properties of myeloid cells. Based on these

findings, we speculate that the progenies of M-medium-treated c-Kit^{+}CD24^{+} NK cells were not NK cells with an altered phenotype, but lineage-converted myeloid cells. Moreover, the absence of EYFP^{+} myeloid progenitors in the *Ncr1*$^{iCRE/WT}$*R26R*$^{EYFP/WT}$ fate-mapping mice suggests the transdifferentiation of NK cells into myeloid cells. Consistent with this finding, the production of myeloid cells from c-Kit^{+}CD24^{+} NK cells only took several days unlike the time-consuming lineage reprogramming with dedifferentiation, which requires several weeks [67,68]. These results support that the lineage conversion of c-Kit^{+}CD24^{+} NK cells into myeloid cells is a process of direct lineage reprogramming which does not involve de-differentiation of the NK cells into myeloid progenitors.

In my studies, almost all experimental data were double-checked using NK cells from two inbred mouse strains (C57BL/6 and BALB/c), with the exception of experiments utilizing transgenic mice. Although there are several differences in hematopoiesis between the two mouse strains, myeloid cell development from c-Kit^{+}CD24^{+} NK cells proceeded independently of mouse strain.

Myeloid/NK cell precursor acute leukemia (MNKPL) and myeloid/NK cell acute leukemia (MNKL) characterized by coexpression of myeloid and NK cell antigens have been reported [69-71]. However, the causes and cellular

origin of the mixed phenotype MNKPL/MNKL are poorly understood due to the rarity of the leukemias. I also found that most of the $EYFP^+$ myeloid cells expressed NK1.1 and NKp46 in *Ncr1*$^{iCRE/WT}$*R26R*$^{EYFP/WT}$ mice. Additionally, some of myeloid cells generated from transferred NK cells *in vivo* still expressed NK1.1. These results might be due to the short lifespan of myeloid cells and *in vivo* environment that can support and maintain NK cells as well as induce differentiation of NK cells into myeloid cells. My findings might suggest that the differentiation of NK cells into myeloid cells could be one of the causes of mixed phenotype acute leukemias.

Here I showed a naturally occurring differentiation of NK cells into myeloid cells in a physiologically relevant experimental settings including steady state as well as the tumor microenvironment using *Ncr1*$^{iCRE/WT}$*R26R*$^{EYFP/WT}$ fate-mapping mice. Although the degree of contribution of NK-to-myeloid cell differentiation in the total myeloid cell pool was low, their existence was clearly demonstrated in an NK cell-depleting study. In addition, I suggested c-Kit and CD24 as additional markers for NK cell subsets with myeloid potential. c-Kit^+CD24^+ NK cells predominantly differentiated into myeloid lineage cells but the myeloid cell production was inhibited by treatment of NK-stimulatory cytokines. I also showed increased NK-derived neutrophils in the myelopoiesis-promoting

tumor environment compared with the steady state. Finally, I identified several transcription factors, such as *Gata2*, *Gfi1b*, *Lmo2*, *Meis1*, *Nfe2*, and *Spi1*, which are involved in differentiation of c-Kit^{+}CD24^{+} NK cells into myeloid cells using RNA sequencing approaches. Based on the RNA sequencing data, I demonstrated that GATA-2 is necessary for the myeloid cell production from c-Kit^{+}CD24^{+} NK cells. Whether differentiation of NK cells into myeloid cells affects the pathogenesis of diseases, such as tumors, infections, autoimmune diseases, injuries, and immunodeficiencies, remains to be determined. In particular, careful approaches will be necessary in anti-cancer therapies using NK cell adoptive transfer. In conclusion, my findings provide deep insight to improve understanding of the developmental pathway of myeloid cells under physiological and pathological conditions.

Summary

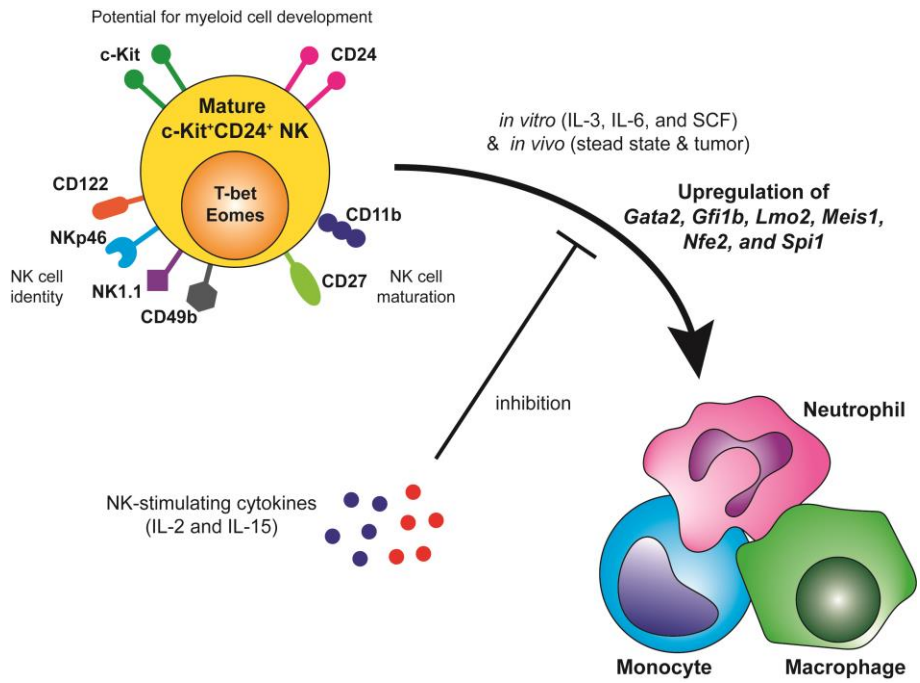

Figure 35. Graphical summary of this study: c-Kit^{+}CD24^{+} NK cells differentiate into myeloid cells in a GATA-2-dependent manner

Among mature CD11b^{+}CD27^{+} NK cells, c-Kit^{+}CD24^{+} NK cells were converted into myeloid cells containing neutrophils, monocyte, and macrophages *in vitro* and *in vivo*. During the conversion, expression of lineage commitment/reprogramming-related transcription factors including GATA-2, Gfi-1b, LMO-2, Meis1, NF-E2, and PU.1 was increased, but IL-2 inhibited the upregulation. I demonstrated that GATA-2 is necessary for the differentiation of c-Kit^{+}CD24^{+} NK cells into myeloid cells.

References

1 Kondo, M., Weissman, I. L. & Akashi, K. Identification of Clonogenic Common Lymphoid Progenitors in Mouse Bone Marrow. *Cell* **91**, 661-672, doi:https://doi.org/10.1016/S0092-8674(00)80453-5 (1997).

2 Akashi, K., Traver, D., Miyamoto, T. & Weissman, I. L. A clonogenic common myeloid progenitor that gives rise to all myeloid lineages. *Nature* **404**, 193-197, doi:10.1038/35004599 (2000).

3 Seita, J. & Weissman, I. L. Hematopoietic stem cell: self-renewal versus differentiation. *Wiley Interdiscip Rev Syst Biol Med* **2**, 640-653, doi:10.1002/wsbm.86 (2010).

4 Avgustinova, A. & Benitah, S. A. Epigenetic control of adult stem cell function. *Nat Rev Mol Cell Biol* **17**, 643-658, doi:10.1038/nrm.2016.76 (2016).

5 Ackermann, M., Liebhaber, S., Klusmann, J. H. & Lachmann, N. Lost in translation: pluripotent stem cell-derived hematopoiesis. *EMBO Mol Med* **7**, 1388-1402, doi:10.15252/emmm.201505301 (2015).

6 Graf, T. Differentiation plasticity of hematopoietic cells. *Blood* **99**, 3089 (2002).

7 Xie, H., Ye, M., Feng, R. & Graf, T. Stepwise Reprogramming of B Cells into Macrophages. *Cell* **117**, 663-676, doi:10.1016/S0092-8674(04)00419-2 (2004).

8 Bussmann, L. H. *et al.* A robust and highly efficient immune cell reprogramming system. *Cell Stem Cell* **5**, 554-566, doi:10.1016/j.stem.2009.10.004 (2009).

9 Cirovic, B. *et al.* C/EBP-Induced Transdifferentiation Reveals Granulocyte-Macrophage Precursor-like Plasticity of B Cells. *Stem Cell Reports* **8**, 346-359, doi:10.1016/j.stemcr.2016.12.015 (2017).

10 Cobaleda, C., Jochum, W. & Busslinger, M. Conversion of mature B cells into T cells by dedifferentiation to uncommitted progenitors. *Nature* **449**, 473-477, doi:10.1038/nature06159 (2007).

11 Laiosa, C. V., Stadtfeld, M., Xie, H., de Andres-Aguayo, L. & Graf, T. Reprogramming of committed T cell progenitors to macrophages and dendritic cells by C/EBP alpha and PU.1 transcription factors. *Immunity* **25**, 731-744, doi:10.1016/j.immuni.2006.09.011 (2006).

12 Hu, T., Murdaugh, R. & Nakada, D. Transcriptional and Microenvironmental Regulation of Lineage Ambiguity in Leukemia. *Front Oncol* **7**, 268, doi:10.3389/fonc.2017.00268 (2017).

13 Park, Y. J. *et al.* Tumor microenvironmental conversion of natural killer cells into myeloid-derived suppressor cells. *Cancer Res* **73**, 5669-5681, doi:10.1158/0008-5472.CAN-13-0545 (2013).

14 Wynn, T. A. Myeloid-cell differentiation redefined in cancer. *Nat Immunol* **14**, 197-199, doi:10.1038/ni.2539 (2013).

15 Biasco, L. *et al.* In Vivo Tracking of Human Hematopoiesis Reveals Patterns of Clonal Dynamics during Early and Steady-State Reconstitution Phases. *Cell Stem Cell* **19**, 107-119, doi:10.1016/j.stem.2016.04.016 (2016).

16 Grzywacz, B. *et al.* Natural killer-cell differentiation by myeloid progenitors. *Blood* **117**, 3548-3558, doi:10.1182/blood-2010-04-281394 (2011).

17 Chen, Q. *et al.* Delineation of Natural Killer Cell Differentiation from Myeloid Progenitors in Human. *Sci Rep* **5**, 15118, doi:10.1038/srep15118 (2015).

18 Becher, B. *et al.* High-dimensional analysis of the murine myeloid cell system. *Nat Immunol* **15**, 1181-1189, doi:10.1038/ni.3006 (2014).

19 Narni-Mancinelli, E. *et al.* Fate mapping analysis of lymphoid cells expressing the NKp46 cell surface receptor. *Proc Natl Acad Sci U S A* **108**, 18324-18329, doi:10.1073/pnas.1112064108 (2011).

20 Hayakawa, Y. & Smyth, M. J. CD27 Dissects Mature NK Cells into Two Subsets with Distinct Responsiveness and Migratory Capacity. *The Journal of Immunology* **176**, 1517-1524, doi:10.4049/jimmunol.176.3.1517 (2006).

21 Thoren, L. A. *et al.* Kit Regulates Maintenance of Quiescent Hematopoietic Stem Cells. *The Journal of Immunology* **180**, 2045-2053, doi:10.4049/jimmunol.180.4.2045 (2008).

22 Kent, D. *et al.* Regulation of hematopoietic stem cells by the steel factor/KIT signaling pathway. *Clin Cancer Res* **14**, 1926-1930, doi:10.1158/1078-0432.CCR-07-5134 (2008).

23 Saenz, S. A. *et al.* IL25 elicits a multipotent progenitor cell population that promotes T(H)2 cytokine responses. *Nature* **464**, 1362-1366, doi:10.1038/nature08901 (2010).

24 Redecke, V. *et al.* Hematopoietic progenitor cell lines with myeloid and lymphoid potential. *Nat Methods* **10**, 795-803, doi:10.1038/nmeth.2510 (2013).

25 Shakiba, N. *et al.* CD24 tracks divergent pluripotent states in mouse and human cells. *Nat Commun* **6**, 7329, doi:10.1038/ncomms8329 (2015).

26 Collier, A. J. *et al.* Comprehensive Cell Surface Protein Profiling Identifies Specific Markers of Human Naive and Primed Pluripotent States. *Cell Stem Cell* **20**, 874-890 e877, doi:10.1016/j.stem.2017.02.014 (2017).

27 Pradier, A. *et al.* Peripheral blood CD56(bright) NK cells respond to stem cell factor and adhere to its membrane-bound form after upregulation of c-kit. *Eur J Immunol* **44**, 511-520, doi:10.1002/eji.201343868 (2014).

28 Terme, M. *et al.* Cancer-induced immunosuppression: IL-18-elicited immunoablative NK cells. *Cancer Res* **72**, 2757-2767, doi:10.1158/0008-5472.CAN-11-3379 (2012).

29 Ehlers, M. *et al.* Immunoregulatory natural killer cells suppress autoimmunity by down-regulating antigen-specific CD8+ T cells in mice. *Endocrinology* **153**, 4367-4379, doi:10.1210/en.2012-1247 (2012).

30 Cichocki, F., Sitnicka, E. & Bryceson, Y. T. NK cell development and function--plasticity and redundancy unleashed. *Semin Immunol* **26**, 114-126, doi:10.1016/j.smim.2014.02.003 (2014).

31 Moignard, V. *et al.* Characterization of transcriptional networks in blood stem and progenitor cells using high-throughput single-cell gene expression analysis. *Nat Cell Biol* **15**, 363-372, doi:10.1038/ncb2709 (2013).

32 Goode, D. K. *et al.* Dynamic Gene Regulatory Networks Drive Hematopoietic Specification and Differentiation. *Dev Cell* **36**, 572-587, doi:10.1016/j.devcel.2016.01.024 (2016).

33 Gao, X. *et al.* Gata2 cis-element is required for hematopoietic stem cell generation in the mammalian embryo. *J Exp Med* **210**, 2833-2842, doi:10.1084/jem.20130733 (2013).

34 Yu, L. *et al.* Reducing Inflammatory Cytokine Production from Renal Collecting Duct Cells by Inhibiting GATA2 Ameliorates Acute Kidney Injury. *Mol Cell Biol* **37**, doi:10.1128/MCB.00211-17 (2017).

35 Lui, J. B., Devarajan, P., Teplicki, S. A. & Chen, Z. Cross-differentiation from the CD8 lineage to CD4 T cells in the gut-associated microenvironment with a nonessential role of microbiota. *Cell Rep* **10**, 574-585, doi:10.1016/j.celrep.2014.12.053 (2015).

36 Youn, J. I. *et al.* Epigenetic silencing of retinoblastoma gene regulates pathologic differentiation of myeloid cells in cancer. *Nat Immunol* **14**, 211-220, doi:10.1038/ni.2526 (2013).

37 Gao, Y. *et al.* Tumor immunoevasion by the conversion of effector NK cells into type 1 innate lymphoid cells. *Nat Immunol* **18**, 1004-1015, doi:10.1038/ni.3800 (2017).

38 Cortez, V. S. *et al.* SMAD4 impedes the conversion of NK cells into ILC1-like cells by curtailing non-canonical TGF-beta signaling. *Nat Immunol* **18**, 995-1003, doi:10.1038/ni.3809 (2017).

39 Park, E. *et al.* Toxoplasma gondii infection drives conversion of NK cells into ILC1-like cells. *Elife* **8**, doi:10.7554/eLife.47605 (2019).

40 Benson, D. M., Jr. *et al.* Stem cell factor and interleukin-2/15 combine to enhance MAPK-mediated proliferation of human natural killer cells. *Blood* **113**, 2706-2714, doi:10.1182/blood-2008-05-159285 (2009).

41 Carson, W. E., Haldar, S., Baiocchi, R. A., Croce, C. M. & Caligiuri, M. A. The c-kit ligand suppresses apoptosis of human natural killer cells through the upregulation of bcl-2. *Proceedings of the National Academy of Sciences of the United States of America* **91**, 7553-7557 (1994).

42 Colucci, F. & Di Santo, J. P. The receptor tyrosine kinase c-kit provides a critical signal for survival, expansion, and maturation of mouse natural killer cells. *Blood* **95**, 984 (2000).

43 Fang, X., Zheng, P., Tang, J. & Liu, Y. CD24: from A to Z. *Cell Mol Immunol* **7**, 100-103, doi:10.1038/cmi.2009.119 (2010).

44 Ayre, D. C. & Christian, S. L. CD24: A Rheostat That Modulates Cell Surface Receptor Signaling of Diverse Receptors. *Front Cell Dev Biol* **4**, 146, doi:10.3389/fcell.2016.00146 (2016).

45 Márquez, C. *et al.* Identification of a Common Developmental Pathway for Thymic Natural Killer Cells and Dendritic Cells. *Blood* **91**, 2760 (1998).

46 Bell, J. J. & Bhandoola, A. The earliest thymic progenitors for T cells possess myeloid lineage potential. *Nature* **452**, 764-767, doi:10.1038/nature06840 (2008).

47 Wada, H. *et al.* Adult T-cell progenitors retain myeloid potential. *Nature* **452**, 768-772, doi:10.1038/nature06839 (2008).

48 Montecino-Rodriguez, E., Leathers, H. & Dorshkind, K. Bipotential B-macrophage progenitors are present in adult bone marrow. *Nature Immunology* **2**, 83-88, doi:10.1038/83210 (2001).

49 Abel, A. M., Yang, C., Thakar, M. S. & Malarkannan, S. Natural Killer Cells: Development, Maturation, and Clinical Utilization. *Front Immunol* **9**, 1869, doi:10.3389/fimmu.2018.01869 (2018).

50 Chiossone, L. *et al.* Maturation of mouse NK cells is a 4-stage developmental program. *Blood* **113**, 5488-5496, doi:10.1182/blood-2008-10-187179 (2009).

51 Robinette, M. L. *et al.* Transcriptional programs define molecular characteristics of innate lymphoid cell classes and subsets. *Nat Immunol* **16**, 306-317, doi:10.1038/ni.3094 (2015).

52 Spits, H., Bernink, J. H. & Lanier, L. NK cells and type 1 innate lymphoid cells: partners in host defense. *Nat Immunol* **17**, 758-764, doi:10.1038/ni.3482 (2016).

53 Peng, H. & Tian, Z. Diversity of tissue-resident NK cells. *Semin Immunol* **31**, 3-10, doi:10.1016/j.smim.2017.07.006 (2017).

54 Simoni, Y. *et al.* Human Innate Lymphoid Cell Subsets Possess Tissue-Type Based Heterogeneity in Phenotype and Frequency. *Immunity* **46**, 148-161, doi:10.1016/j.immuni.2016.11.005 (2017).

55 Vivier, E. *et al.* Innate Lymphoid Cells: 10 Years On. *Cell* **174**, 1054-1066, doi:10.1016/j.cell.2018.07.017 (2018).

56 Theurich, S. *et al.* IL-6/Stat3-Dependent Induction of a Distinct, Obesity-Associated NK Cell Subpopulation Deteriorates Energy and Glucose Homeostasis. *Cell Metab* **26**, 171-184 e176, doi:10.1016/j.cmet.2017.05.018 (2017).

57 Blasius, A. L., Barchet, W., Cella, M. & Colonna, M. Development and function of murine B220+CD11c+NK1.1+ cells identify them as a subset of NK cells. *J Exp Med* **204**, 2561-2568, doi:10.1084/jem.20070991 (2007).

58 Filipovic, I. *et al.* Molecular definition of group 1 innate lymphoid cells in the mouse uterus. *Nat Commun* **9**, 4492, doi:10.1038/s41467-018-06918-3 (2018).

59 Loyon, R. *et al.* IL-21-Induced MHC Class II+ NK Cells Promote the Expansion of Human Uncommitted CD4+ Central Memory T Cells in a Macrophage Migration Inhibitory Factor-Dependent Manner. *J Immunol* **197**, 85-96, doi:10.4049/jimmunol.1501147 (2016).

60 Nakayama, M. *et al.* Natural killer (NK)-dendritic cell interactions generate MHC class II-dressed NK cells that regulate CD4+ T cells. *Proc Natl Acad Sci U S A* **108**, 18360-18365, doi:10.1073/pnas.1110584108 (2011).

61 Omi, A., Enomoto, Y., Kiniwa, T., Miyata, N. & Miyajima, A. Mature resting Ly6C(high) natural killer cells can be reactivated by IL-15. *Eur J Immunol* **44**, 2638-2647, doi:10.1002/eji.201444570 (2014).

62 Kang, H. *et al.* GATA2 Is Dispensable for Specification of Hemogenic Endothelium but Promotes Endothelial-to-Hematopoietic Transition. *Stem Cell Reports* **11**, 197-211, doi:10.1016/j.stemcr.2018.05.002 (2018).

63 Pereira, C. F. *et al.* Induction of a hemogenic program in mouse fibroblasts. *Cell Stem Cell* **13**, 205-218, doi:10.1016/j.stem.2013.05.024 (2013).

64 Batta, K., Florkowska, M., Kouskoff, V. & Lacaud, G. Direct reprogramming of murine fibroblasts to hematopoietic progenitor cells. *Cell Rep* **9**, 1871-1884, doi:10.1016/j.celrep.2014.11.002 (2014).

65 Pulecio, J. *et al.* Direct Conversion of Fibroblasts to Megakaryocyte Progenitors. *Cell Rep* **17**, 671-683, doi:10.1016/j.celrep.2016.09.036 (2016).

66 Xu, J., Du, Y. & Deng, H. Direct lineage reprogramming: strategies, mechanisms, and applications. *Cell Stem Cell* **16**, 119-134, doi:10.1016/j.stem.2015.01.013 (2015).

67 Vierbuchen, T. & Wernig, M. Direct lineage conversions: unnatural but useful? *Nat Biotechnol* **29**, 892-907, doi:10.1038/nbt.1946 (2011).

68 Cieslar-Pobuda, A. *et al.* Transdifferentiation and reprogramming: Overview of the processes, their similarities and differences. *Biochim Biophys Acta Mol Cell Res* **1864**, 1359-1369, doi:10.1016/j.bbamcr.2017.04.017 (2017).

69 Suzuki, R. *et al.* CD7⁺ and CD56⁺ Myeloid/Natural Killer Cell Precursor Acute Leukemia: A Distinct Hematolymphoid Disease Entity. *Blood* **90**, 2417 (1997).

70 Suzuki, R. & Nakamura, S. Malignancies of natural killer (NK) cell precursor: myeloid/NK cell precursor acute leukemia and blastic NK cell lymphoma/leukemia. *Leukemia Research* **23**, 615-624, doi:https://doi.org/10.1016/S0145-2126(98)00194-5 (1999).

71 Chen, B., Xu, X., Ji, M. & Lin, G. Myeloid/NK cell acute leukemia. *Int J Hematol* **89**, 365-367, doi:10.1007/s12185-009-0282-9 (2009).

국문 초록

일부 연구를 통해 질병이나 면역 세포 분화 관련 물질의 인위적인 발현 조절 상황에서 골수성 계통이 아닌 세포에서 골수성 세포가 생성될 수 있음이 밝혀졌지만, 정상 상황에서 골수성 전구 세포는 체내 골수성 세포를 생성하는 유일한 세포로 알려져 있다. 본 연구실에서는 암 환경에서 성숙한 $CD11b^{+}CD27^{+}$ 자연 살해 세포가 골수성 면역 억제 세포로 분화할 수 있음을 밝힌 바 있다. 이 연구는 정상 상황에서의 자연 살해 세포의 골수성 세포로의 전환, 골수성 세포로 전환 가능한 자연 살해 세포의 아형과 전환의 핵심 조절 인자를 규명하기 위해 진행되었다.

우선 자연 살해 세포를 추적할 수 있는 유전자 조작 마우스를 통해 자연 살해 세포에서 유래된 것으로 추정되는 골수성 세포가 정상 상황과 암 상황에서 존재함을 확인하였다. 이후 RNA sequencing 과 *in vitro* culture experiment 를 통해 $CD11b^{+}CD27^{+}$ 자연 살해 세포 중 c-Kit 과 CD24 를 발현하는 세포만이 골수성 세포로 전환되며, 자연 살해 세포 활성화 사이토카인에 의해 전환이 억제됨을 밝혔다. 또한 $c\text{-}Kit^{+}CD24^{+}$ 자연 살해 세포를 마우스에 주입하는 adoptive cell transfer 실험을 통해 $c\text{-}Kit^{+}CD24^{+}$ 자연 살해 세포가 체내에서도 골수성 세포로 분화할 수 있음을 확인하였다. 다음으로 RNA sequencing 과 유세포 분석을 진행하여 골수성

세포로 분화할 수 있는 c-Kit$^+$CD24$^+$ 자연 살해 세포의 특성을 확인한 결과, c-Kit$^+$CD24$^+$ 자연 살해 세포는 다른 자연 살해 세포군과 마찬가지로 자연 살해 세포 특이적인 발현 패턴을 가지고 있으며 IFN-γ 와 CD107a 을 다른 자연 살해 세포군보다도 더 많이 생성할 수 있음을 확인하여, c-Kit$^+$CD24$^+$ 자연 살해 세포가 골수성 세포로의 분화 가능성을 가지고 있는 자연 살해 세포임을 밝혔다. 마지막으로 c-Kit$^+$CD24$^+$ 자연 살해 세포의 골수성 세포로의 분화 과정에 관여하는 핵심 조절 인자를 규명하기 위해 RNA sequencing 을 진행하여 GATA-2, Gfi-1b, LMO-2 과 PU.1 등 다양한 전사 인자가 관여함을 확인하였다. 이들 중 면역 세포의 계통 결정에 중요한 역할을 하는 것으로 알려진 GATA-2 에 초점을 맞춰 이후 GATA-2 억제제 처리 및 GATA-2 과발현 실험을 진행한 결과, GATA-2 가 c-Kit$^+$CD24$^+$ 자연 살해 세포가 골수성 세포로의 분화에 필요함을 밝혔다. 따라서 본 연구를 통해 체내 골수성 세포를 생성하는 과정으로 GATA-2 에 의존적인 c-Kit$^+$CD24$^+$ 자연 살해 세포의 골수성 세포로의 분화를 새롭게 규명할 수 있었다.

주요어: 직접교차분화, 골수성 세포 발달, 자연 살해 세포, c-Kit, CD24, GATA-2

학 번: 2011-24245